JEM Journal of Experimental Medicine

ARTICLE

γδ T cell profiling in a cohort of preterm infants reveals elevated frequencies of *CD83*⁺ γδ T cells in sepsis

Ximena León-Lara[1], Alina S. Fichtner[1], Maike Willers[2], Tao Yang[1], Katharina Schaper[1], Lennart Riemann[1,2], Jennifer Schöning[3], Anna Harms[1], Vicente Almeida[1], Anja Schimrock[1], Anika Janssen[1], Laura Ospina-Quintero[1], Constantin von Kaisenberg[4], Reinhold Förster[1,6], Matthias Eberl[7,8], Manuela F. Richter[5], Sabine Pirr[2], Dorothee Viemann[2,3,6,9,10]*, and Sarina Ravens[1,6]*

Preterm infants are at high risk of developing neonatal sepsis. γδ T cells are thought to be an important set of effector cells in neonates. Here, γδ T cells were investigated in a longitudinal cohort of preterm neonates using next-generation sequencing, flow cytometry, and functional assays. During the first year of life, the Vγ9Vδ2 T cell subset showed dynamic phenotypic changes and elevated levels of fetal-derived Vγ9Vδ2 T cells were evident in infants with sepsis. Single-cell transcriptomics identified *HLA-DR*^{hi} *CD83*⁺ γδ T cells in neonatal sepsis, which expressed genes related to antigen presentation. In vitro assays showed that CD83 was expressed on activated Vγ9Vδ2 T cells in preterm and term neonates, but not in adults. In contrast, activation of adult Vγ9Vδ2 T cells enhanced CD86 expression, which was presumably the key receptor to induce CD4 T cell proliferation. Together, we provide a map of the maturation of γδ T cells after preterm birth and highlight their phenotypic diversity in infections.

Introduction

Neonatal sepsis is a life-threatening disease; preterm neonates are the most vulnerable group (van der Poll et al., 2021). Neonates born before 32 wk of gestation are considered physiologically and immunologically immature. In addition, the reduced transfer of maternal immunity due to frequently delayed breast milk supply and a common need for organ support via invasive medical devices increase particularly their risk of late-onset sepsis (LOS). The incidence of LOS usually peaks in the second week of life and is in the majority of cases caused by *Staphylococcus* species (spp.), *Escherichia coli*, and *Candida* spp. following environmental exposure (Kan et al., 2016).

Human γδ T cells are among the first T cells generated in the early fetal thymus and begin to develop around 7–9 wk of gestation (McVay et al., 1998). They become preprogrammed effector cells during intrathymic development and have been described to respond to a variety of infections in utero (Cairo et al., 2014; Ma et al., 2021; Vermijlen et al., 2010). After the transition from the relatively sterile environment in utero, the newborn's immune system is exposed to a number of environmental signals. These must be tolerated by the immune system and continue to induce immune cell adaptation at the population and individual immune subset levels throughout the first weeks and months of life (Kan et al., 2016; Olin et al., 2018; Torow et al., 2023).

In this context, it has been described that fetal thymus-derived γδ T cells immediately expand after birth (Papadopoulou et al., 2020; Ravens et al., 2020). In fact, due to their early-life ontogeny and high responsiveness at birth (Gibbons et al., 2009; Sanchez et al., 2023), they are thought to be an important effector T cell subset in infants. However, there are only a few studies on γδ T cells in neonatal and infant viral or bacterial infections (Guo et al., 2018; Rahman Qazi et al., 2021; Tuengel et al., 2021). Furthermore, the underlying responsiveness and origin of human γδ T cells in neonatal sepsis are unknown.

Human γδ T cells express a T cell receptor (TCR) that is composed of the γ-chain (TRG) and the δ-chain (TRD) generated

[1]Institute of Immunology, Hannover Medical School, Hannover, Germany; [2]Department of Pediatric Pneumology, Allergology and Neonatology, Hannover Medical School, Hannover, Germany; [3]Translational Pediatrics, Department of Pediatrics, University Hospital Wuerzburg, Wuerzburg, Germany; [4]Department of Obstetrics, Gynecology, and Reproductive Medicine, Hannover Medical School, Hannover, Germany; [5]AUF DER BULT - Children's and Youth Hospital, Hannover, Germany; [6]Cluster of Excellence RESIST (EXC 2155), Hannover Medical School, Hannover, Germany; [7]Division of Infection and Immunity, School of Medicine, Cardiff University, Cardiff, UK; [8]Systems Immunity Research Institute, Cardiff University, Cardiff, UK; [9]PRIMAL (Priming IMmunity at the Beginning of Life) Consortium, Lübeck, Germany; [10]Center for Infection Research, University Würzburg, Würzburg, Germany.

*D. Viemann and S. Ravens contributed equally to this paper. Correspondence to Sarina Ravens: ravens.sarina@mh-hannover.de.

by V(D)J gene rearrangements (Notarangelo et al., 2016). One common way to classify human γδ T cells into functionally and ontogenetically distinct subsets is based on the variable (V) gene region usage of their γδ TCR (Fichtner et al., 2020b). Cells expressing a TCR positive for the Vδ1 chain are classified as adaptive-like γδ T cells. They develop as naïve cells within the postnatal thymus cells, acquire a cytotoxic effector phenotype upon sensing infection, cancer, or stress, and undergo (oligo) clonal expansion, resulting in highly individual Vδ1 T cell signatures in adults (Davey et al., 2017; Di Lorenzo et al., 2019; Ravens et al., 2017; Ribot et al., 2014). Cells expressing a γδ TCR positive for the Vδ2 chain, paired with a Vγ9-chain using the *TRGJP* gene as a joining element, are named Vγ9Vδ2 T cells. Fetal thymic development of γδ T cells is biased towards this subset, with the majority of these Vγ9Vδ2 T cells being preprogrammed to become granzyme A–producing effector cells during intrathymic development (Sanchez et al., 2022; Tan et al., 2021; Tieppo et al., 2020). Moreover, fetal-derived Vγ9Vδ2 T cells are characterized by a specific set of Vγ9$^+$ and Vδ2$^+$ γδ TCR sequences that can be identified by next-generation sequencing (NGS) of the γδ TCR (Papadopoulou et al., 2019).

These Vγ9Vδ2$^+$ TCRs sense and respond to small, nonpeptidic metabolites from the isoprenoid synthesis often referred to as phosphoantigens. The by far most potent phosphoantigen for inducing Vγ9Vδ2 responses is the isopentenyl pyrophosphate and (E)-4-hydroxy-3-methyl-but-2-enyl pyrophosphate (HMBPP) compound (Eberl et al., 2003; Herrmann and Karunakaran, 2022; Morita et al., 2007). The HMBPP is derived from a variety of microbes, including bacteria or the common microbiota, but is not produced by higher eukaryotes including humans (Eberl et al., 2003). Accordingly, Vγ9Vδ2 T cells may represent an important set of highly responsive effector cells for detecting bacterial infections in susceptible preterm neonates. Furthermore, the recent identification of type 2 and type 3 Vγ9Vδ2 effector T cells by NGS approaches in the steady-state fetal thymus and other studies (Sanchez Sanchez et al., 2022; Tan et al., 2021; Vermijlen et al., 2007) suggests pleiotropic functional capabilities of human γδ T cells with implications for immune homeostasis or surveillance in early life.

Here, in-depth monitoring of peripheral blood γδ T cells in a longitudinal cohort of preterm neonates reveals dynamic maturation patterns of Vγ9Vδ2 and Vδ1 T cell subsets, largely attributable to age during the first year of life. Importantly, in neonatal sepsis, a polyclonal expansion of Vγ9Vδ2 T cells was identified with increased expression for *CD83* and other molecules relating to antigen presentation. In vitro assays confirmed upregulation of HLA-DR and CD83 on HMBPP-activated Vγ9Vδ2 T cells in preterm and term neonates, but not in adults. The acquisition of CD83 on neonatal Vγ9Vδ2 T cells suggests a functional diversity of γδ T cells in infectious diseases in infancy.

Results

Increased frequencies of Vγ9Vδ2 T cells are found in premature infants with neonatal sepsis

Peripheral blood γδ T cells were studied in a longitudinal cohort of 100 preterm neonates at four time points, namely 1–14 days, 21–35 days, 6–10 mo, and 13–19 mo after birth (Table 1) (Marißen et al., 2019). Initial flow cytometry analysis in 100 preterm children showed an increase in the frequency of Vγ9 T cells, representing the majority of Vγ9Vδ2 T cells (Davey et al., 2018), and Vδ1 T cells among CD3 T cells with increasing age, while specifically Vγ9 T cells expanded within the first month of life (Fig. S1, A and B).

A quarter of the preterm infants in our study population were diagnosed with neonatal sepsis, and 64% of these had microbiologically confirmed bloodstream infections (Table 1). Both clinical and microbiologically confirmed sepsis diagnosed during the first 30 days of life were included as neonatal sepsis. The period of sepsis was considered as the time of sepsis diagnosis and up to 28 days after the initial diagnosis. More than 2 mo after the initial diagnosis was considered a sepsis-free period.

Table 1. **Demographic and clinical characteristics of participants**

Characteristic	All infants (*n* = 100)
Sample collection	
0–14 days, no. (%)	71 (71)
21–35 days, no. (%)	94 (94)
6–9 mo, no. (%)	77 (77)
13–19 mo, no. (%)	66 (66)
Gestational age at delivery	
Median, wk (min–max)	30.4 (23.1–32.5)
Degree prematurity	
Extreme (<28 wk), no. (%)	25 (25)
Early (28.1–32 wk), no. (%)	57 (57)
Moderate (32.1–34 wk), no. (%)	18 (18)
Birthweight, grams median (min–max)	1,310 (520–2,100)
Female, no. (%)	52 (52)
Delivery by caesarean section, no. (%)	76 (76)
Singleton gestation, no. (%)	52 (52)
APGAR score at 5 min, median (min–max)	8 (5–10)
APGAR score at 10 min, median (min–max)	9 (7–10)
Antenatal corticosteroids, no. (%)	97 (97)
Maternal antibiotics 48 h before birth, no. (%)	74 (74)
Antibiotics in the first 30 days of life, no. (%)[a]	43 (43)
AIS, no. (%)	27 (27)
Meconium plug syndrome, no. (%)	10 (10)
Neonatal pneumonia, no. (%)	1 (1)
Necrotizing enterocolitis	3 (3)
Bronchopulmonary dysplasia	19 (19)
Sepsis in the first 30 days of life, no. (%)	25 (25)
Age at diagnosis, days median (min–max)	8 (1–30)
Positive blood culture[b]	16
Length of postnatal hospital stay, days median (min–max)	51 (21–190)
Days in neonatal intensive care unit, median (min–max)	22 (0–91)

[a]Includes treatment of cases with suspected and confirmed infection.
[b]Blood culture–proven sepsis: four *Staphylococcus epidermis*, three *Staphylococcus aureus*, two *S. aureus*/*S. epidermis*, five *Staphylococcus capitis*, one *Serratia marcescens*, one *Bacillus cereus*.

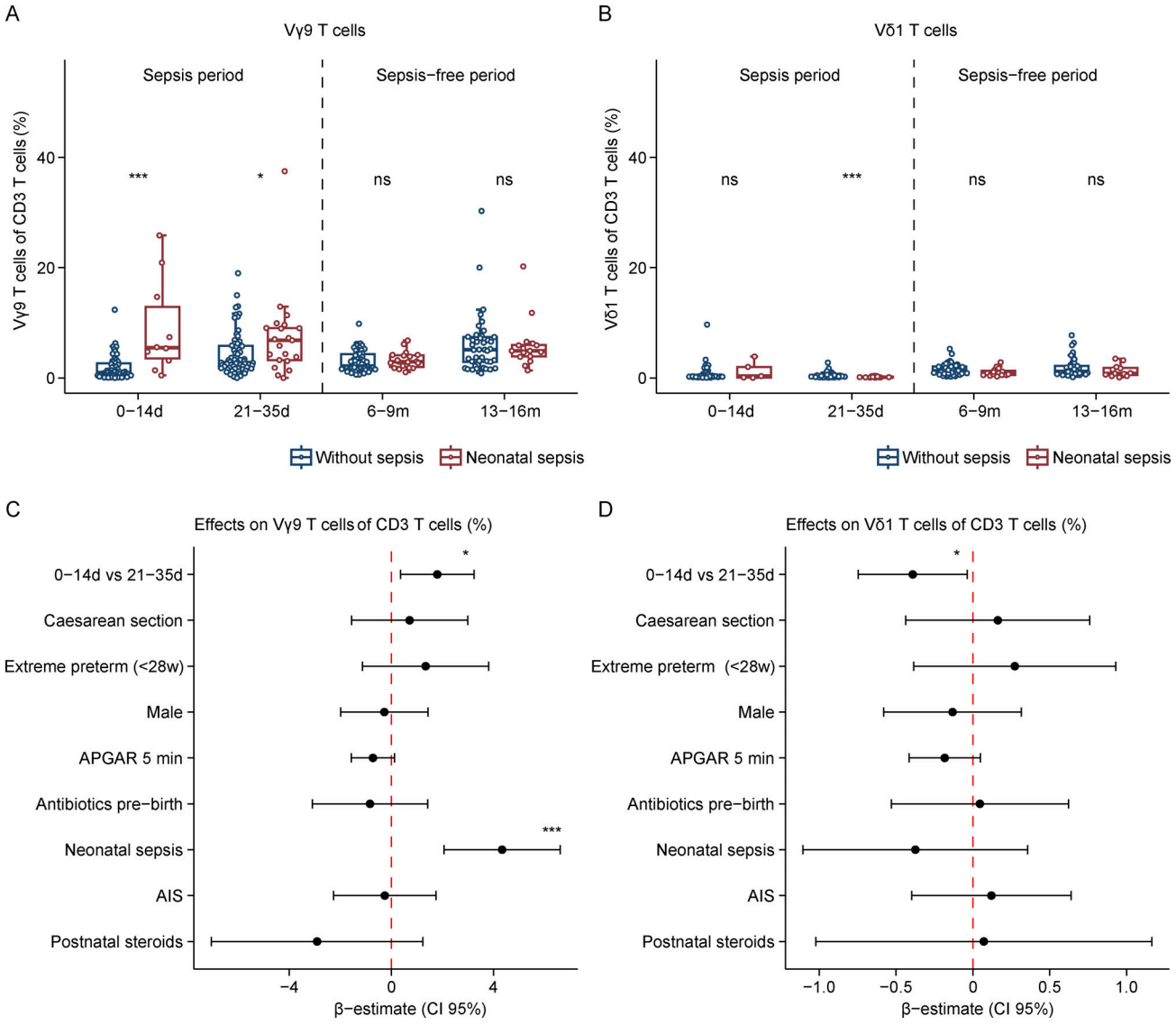

Figure 1. **Sepsis results in increased Vγ9 T cell frequencies in preterm infants. (A and B)** Box plots of the frequency of (A) Vγ9 T cells or (B) Vδ1 T cells among CD3 T cells by FACS during the first 0–14 days (d), 21–35 days, 6–9 mo (m), and 13–16 mo after birth in relation to the diagnosis of sepsis during the neonatal period. **(C and D)** Forest plots of the β-estimates ± 95% confidence intervals of the indicated variables on the frequency of (C) Vγ9 T cells or (D) Vδ1 T cells among CD3 T cells during the first month of life. The vertical dotted red line indicates null effect. P values were determined by Mann–Whitney *U* test (A and B) or linear mixed-effects modeling (C and D); ns = not significant, *P < 0.05, ***P < 0.001.

Importantly, during the period of sepsis, the frequency of Vγ9 T cells in the first month of life, but not of Vδ1 T cells, among CD3 T lymphocytes (Fig. 1, A and B) and also among all γδ T cells (Fig. S1 C) was elevated in the sepsis patients. In the sepsis-free period, no difference in the frequency of Vγ9 T cells was observed between children with a history of neonatal sepsis and those without sepsis (Fig. 1 A). Lymphocyte count information was obtained for the time points during the timeframe of sepsis, and samples were collected at 1–14 days of age and 21–35 days of age, when available. Among those, 1 of 5 (20%) neonates with sepsis and 7 of 22 (31.8%) neonates without sepsis had lymphocyte counts below the reference values during the first 14 days of life. At 21–35 days of age, 3 of 11 (27.3%) neonates with sepsis and 1 of 40 (2.5%) neonates without sepsis had lymphopenia (Fig. S1 D). Of note, no positive correlation was observed between the absolute lymphocyte cell counts and the frequencies of Vγ9 T cells or Vδ1 T cells among CD3 T cells (Fig. S1, E and F). Next, the adjusted effect of neonatal sepsis on the frequency of Vγ9 T cells or Vδ1 T cells among CD3 T cells during the first month of life (period of sepsis) was determined using a linear mixed effect model while controlling for other perinatal factors with a potential impact on the frequency of Vγ9 T cells or Vδ1 T cells as fixed effects. Such potential confounders included extreme prematurity (birth before 28 wk of gestation), caesarean section, administration of antibiotic treatment 48 h prior to birth, diagnosis of amniotic infection syndrome (AIS), and the administration of at least one cycle of postnatal steroid treatment. These analyses provided evidence that the increased Vγ9 T cell frequencies among CD3 T cells within the first month of life was driven by age and was particularly strong when sepsis

occurred (Fig. 1 C). In contrast, the Vδ1 T cell frequency was only influenced by age and not by any of the parameters analyzed (Fig. 1 D).

In conclusion, flow cytometric profiling of peripheral blood T lymphocytes in a longitudinal cohort of preterm neonates revealed elevated levels of Vγ9 T cells in neonatal sepsis.

γδ T cell clones with fetal origin are responsive to neonatal sepsis

To assess changes in the composition of the γδ TCR repertoire after preterm birth, an mRNA-based NGS analysis of the TRD repertoire of FACS-sorted total γδ T cells from peripheral blood cells of 58 longitudinally followed preterm neonates was performed. To further determine differences among preterm and term infants, the publicly available TRD repertoire of total peripheral γδ T cells from five term infants aged 12–24 mo was also included in the analysis (Ravens et al., 2020). Based on the characteristics of the TRD repertoire, fetal-derived γδ T cells can be identified by a low number of random nucleotide additions (N additions) within the gene junctions and preferential use of *TRDJ3* gene elements (Papadopoulou et al., 2019) that overall results in a shared clonal repertoire, named as public TCR repertoire, in neonates. In contrast, postnatal-derived TRD repertoires are enriched for *TRDJ1* gene elements and display a higher number of N additions. Here, a clustering approach considering multiple parameters for individual TCR features, namely *TRDV*, *TRDD*, and *TRDJ* usage, length of the complementarity-determining region-3 (CDR3), N additions, and number of donors sharing each individual clone (occurrences) was carried out, allowing the overall composition of the TRD repertoire to be studied in a joint manner. The unbiased clustering approach of 13,192,322 TRD sequences, obtained from isolated γδ T cells of the 58 preterm neonates at the respective time points and five term infants aged 12–24 mo, resulted in five distinct TRD repertoire clusters (Table S1).

TCR groups 1–3 consisted of public *TRDV2* clones characterized by a low number of nucleotide insertions (0–7). These clusters were enriched during the first 30 days of life, where they represented >50% of the total TRD repertoire (Fig. S2 A). In particular, the TCR group 1 with very low numbers of N additions and preferential use of *TRDJ3* gene elements, previously assigned to fetal-derived γδ T cells (Papadopoulou et al., 2019; Tieppo et al., 2020), increased in frequency during the first 4 wk of life (Fig. S2 A). Later in life, the frequency of these clusters (TCR group 1–3) decreased, but they were still detectable. Notably, the fetal-like TCR groups 1–3 persisted with a similar abundance in the periphery in both preterm infants at 13–16 mo of age and term infants at 12–24 mo of age (Fig. S2 A). This indicates that fetal-derived γδ T cell clones can persist into childhood independent of the prematurity state at birth. Moreover, at 6 mo of age, the abundance of *TRDV1* clones (cluster 4 and 5), defined by longer CDR3 sequences and preferential usage of *TRDJ1* and *TRDJ2* gene elements was increased in all infants compared with earlier time points (Fig. S2 A). These dynamic changes were further illustrated within another TRD repertoire analysis strategy, where the higher occurrence of non-*TRDJ3* clones with more N additions after the early neonatal period (Fig. S2 B), presumably, led to privatization (Fig. S2 C) and diversification (Fig. S2 D) of the TRD repertoire during infancy.

Next, to address the potential responsiveness of fetal-derived Vγ9Vδ2 T cells to neonatal sepsis, the abundance of the five identified TCR clusters at the respective time points after birth was examined in relation to the diagnosis of neonatal sepsis (Fig. 2 A). Of all the clusters, the fetal-derived TCR cluster 1, defined by *TRDV2*$^{+}$, *TRDJ3*^{hi}, and N-additions^{lo}, was enriched in infants with neonatal sepsis. Later on, during the sepsis-free period, no significant difference was observed between sepsis and sepsis-free infants for all five clusters (Fig. 2 A). Next, tree maps representing the composition of the TRD repertoire in an infant diagnosed with neonatal sepsis on day 5 showed polyclonal expansion of γδ T cells upon sepsis, with *TRDV2–TRDJ3* rearranged as predominant (Fig. 2 B). Furthermore, sepsis did not lead to a focus on TRD repertoire in sepsis, as reflected by a similar inverse Simpson index between neonates and infants diagnosed with and without sepsis (Fig. 2 C). Further assessment of the TRG repertoires in another set of experiments suggested a slight increase in *TRGJP* gene element usage in the TRG repertoire of neonates with sepsis as compared with sepsis-free neonates (Fig. S2 E).

In summary, the TRD and TRG repertoire analyses revealed primarily a polyclonal expansion of fetal-derived Vγ9Vδ2 T cells, which is the most prevalent subset in this time window, following sepsis in preterm infants. In addition, sepsis did not induce an expansion of adult-like TCR clusters, suggesting sepsis not being an event triggering extrathymic peripheral selection of postnatal clones.

Age-dependent maturation of γδ T cells during infancy

Next, we aimed to define postnatal maturation traits of γδ T cells in uninfected preterm neonates and those that had sepsis in the neonatal period. Thus, we performed spectral flow cytometry of surface markers associated with different activation stages and effector capabilities of γδ T cells in a subgroup of 38 infants at the four respective time points after birth. Of note, 10 of them were diagnosed with sepsis during the neonatal period. The multicolor antibody panel included five lineage markers including Vγ9, Vδ2, and Vδ1, and 15 phenotypic markers to distinguish different subsets of naïve and effector γδ T cells, which was previously established for human γδ T cells (Barros-Martins et al., 2022). These phenotypic markers range from molecules to distinguish different stages of immune cell differentiation like CCR7, CD27, and CD28, cellular activation such as CD69 and CD57, and natural killer (NK)–associated molecules that include NKG2D and NKG2A, and the chemokine receptor CCR5 expressed on circulating Vγ9Vδ2 T cells (Brandes et al., 2003; Glatzel et al., 2002; Liuzzi et al., 2016). Most importantly, this antibody panel can distinguish naïve, mainly attributed to CD27, CD28, and CCR7, coexpression; diverse sets of type 1 immunity and activated γδ T cells characterized by NKG2A, NKG2D, or CD16; type 2 immunity γδ T cells defined by CCR4 and CD4 coexpression on the surface; and type 3 immunity γδ T cells identified by surface CCR6 and CD161 expression (Sanchez et al., 2022; Tan et al., 2021). In the following analyses, the frequencies

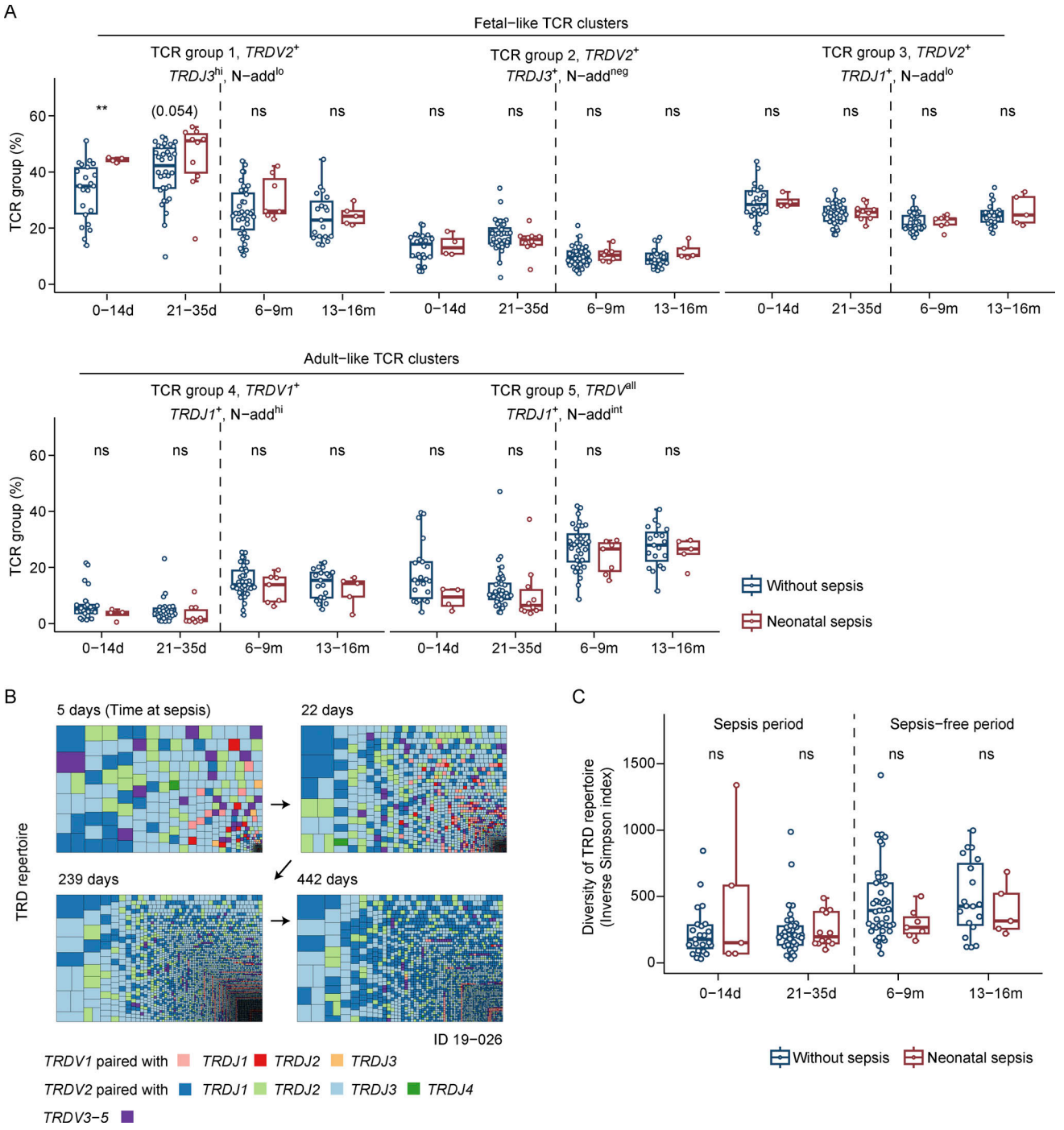

Figure 2. **Polyclonal expansion of *TRDV2*⁺ TRD clones with fetal-like characteristics in neonatal sepsis.** The total TRD repertoire of FACS-sorted γδ T cells from 58 longitudinally followed preterm infants and five term infants was clustered based on V(D)J characteristics, resulting in five TCR groups. **(A)** Frequency of each TCR group at 0–14 days (d), 21–35 days, 6–9 mo (m), or 13–16 mo after preterm birth in relation to the diagnosis of sepsis in the neonatal period. **(B)** Treemaps showing the TRD repertoire diversity in a representative donor diagnosed with sepsis on day 5 after birth. Each box represents one clone, and boxes are sized according to the clone frequency. Each clone (box) is color-coded according to the *TRDV–TRDJ* pairing. **(C)** Diversity index of the TRD repertoire at the indicated time points in relation to the diagnosis of sepsis in the neonatal period. P values were determined by Mann–Whitney *U* test (A and C); ns = not significant, **P < 0.01.

of the defined subsets of naïve, type 2, and type 3 immunity on Vγ9Vδ2 T cells or Vδ1 T cells, as well as the frequencies of NK, activation, and cytotoxicity markers on Vγ9Vδ2 or Vδ1 T cells per donor at the respective time points, were subjected to dimensionally reduced principal component analyses (PCA). Notably, for this analysis, only the 28 longitudinally followed uninfected neonates were considered to first address age-dependent maturation traits of γδ T cells in uninfected neonates. For Vγ9Vδ2 T cells, the visualization of the two principal dimensions of the resulting principal component scores per

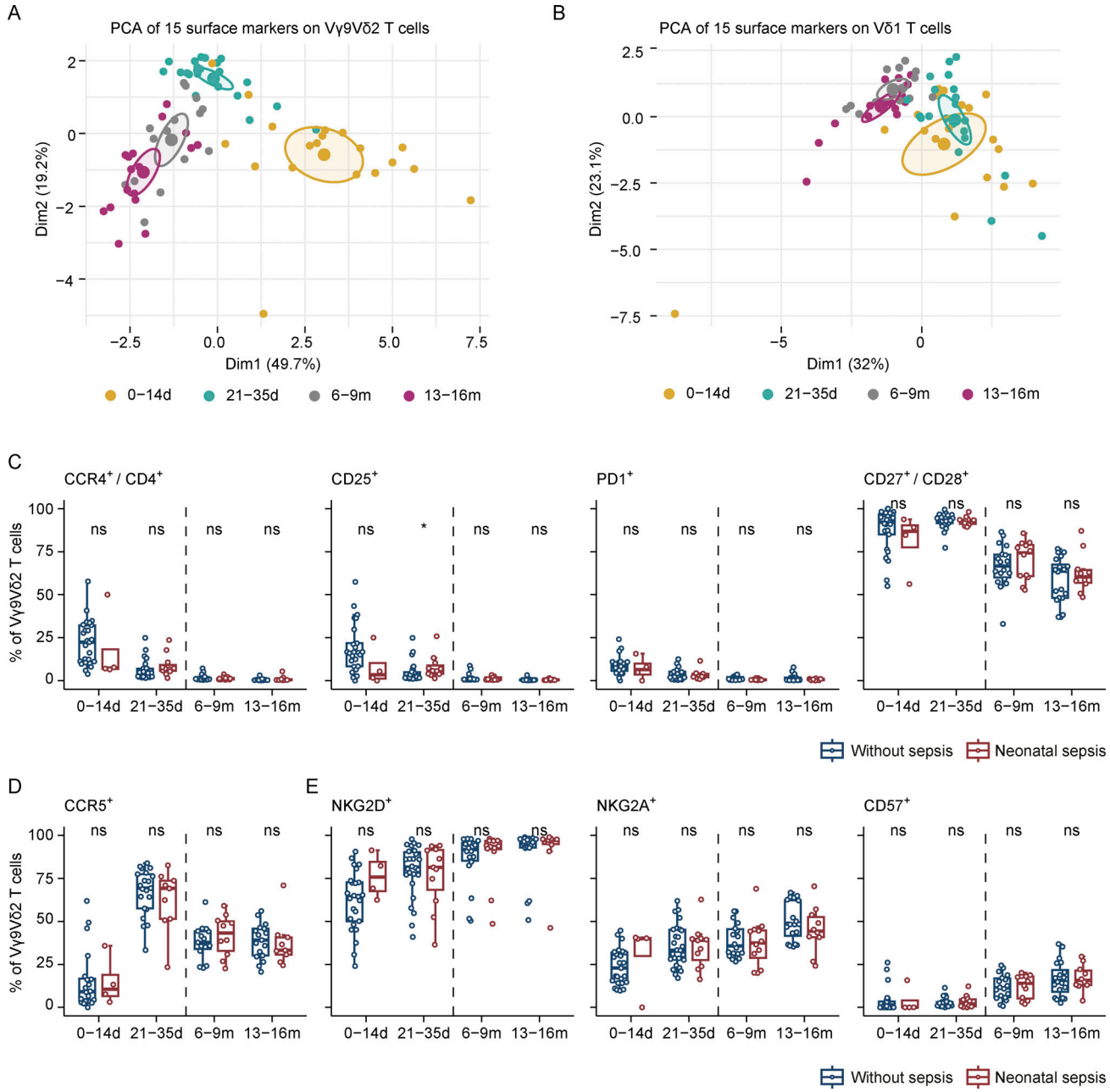

Figure 3. **Age-dependent maturation of γδ T cells during infancy. (A and B)** PCA based on the frequency of positive cells for 15 surface markers on (A) Vγ9Vδ2 or (B) Vδ1 T cells measured by flow cytometry from 28 children without sepsis during the neonatal period. The PCA score plots were color-coded according to the age at sampling. The mean and the 95% confidence ellipses are shown for the corresponding age at sampling. **(C)** Box plots of the frequency of CCR4, CD4 co-expression, CD25, PD1, or CD27, CD28 co-expression on Vγ9Vδ2 T cells per donor by FACS at 0–14 days (d), 21–35 days, 6–9 mo (m), and 13–16 mo after preterm birth in infants diagnosed with and without neonatal sepsis. **(D)** Frequency of CCR5 on Vγ9Vδ2 T cells per donor and time point in relation to the diagnosis of sepsis in the neonatal period. **(E)** Box plots of the frequency of NKG2D, NKG2A, or CD57 on Vγ9Vδ2 T cells per donor and time point in relation to the diagnosis of sepsis in the neonatal period. P values were determined by Mann–Whitney *U* test (C, D, and E); ns = not significant, *P < 0.05.

individual colored by the time of sampling shows that the phenotype composition of Vγ9Vδ2 T cells segregates as a function of age (Fig. 3 A). In particular, the first time point, 0–14 days, clusters away from the other time points. In contrast, Vδ1 T cell PCA scores overlap between time points (Fig. 3 B). For Vγ9Vδ2 T cells, the NK receptors NKG2D and NKG2A, the activation marker CD25, the type 2–like immunity phenotypic markers CCR4 and CD4, as well as the coinhibitory molecule PD-1 contributed most to the dimension 1 of the PCA (Fig. S3 A), whereas the chemokine receptor CCR5, the type III Fcγ receptor CD16, and the coexpression of CD28 and CD27 contributed more to the dimension 2 for Vγ9Vδ2 T cells (Fig. S3 B). For Vδ1 T cells, the coexpression of CCR7 and CD27, as well as the expression of the surface markers CD16, NKG2A, and CD69, were the major contributors to the Vδ1 principal components (Fig. S3, C and D), albeit there were

only minor changes during the first year of life (Fig. S3, E and F).

Next, to determine the potential long-term consequences of neonatal sepsis on postnatal maturation, a manual gating on the respective surface receptors was performed on Vγ9Vδ2 and Vδ1 T cells, respectively. For this, we categorized the spectral flow cytometry data of the 38 preterm infants into those with sepsis (n = 10) and those without neonatal sepsis (n = 28) to compare the frequency of specific surface markers among groups. The CCR4 and CD4 coexpression of Vγ9Vδ2 T cells and the expression of the surface markers CD25 and PD1 on Vγ9Vδ2 T cells were highest in the first month of life and were gradually decreasing with increasing age, with only discrete increase in the activation marker CD25 among those infected during the timeframe of sepsis, namely 21–35 days after birth, which did not persist in later timepoints (Fig. 3 C). In addition, this period was characterized by a higher frequency of Vγ9Vδ2 T cells coexpressing CD27 and CD28, which was used to define less mature Vγ9Vδ2 T cells (Fig. 3 C), as well as by the expression of the chemokine receptor CCR5, in both sepsis and sepsis-free neonates (Fig. 3 D). Furthermore, the NK receptors NKG2D and NKG2A, and the surface marker CD57, which were important contributors to the PCA of Vγ9Vδ2 T cells PCA dimensions (Fig. S3, A and B), showed a progressive surface acquisition on Vγ9Vδ2 T cells within the first year of life, and this was independent of sepsis (Fig. 3 E). Similarly, the surface phenotype of Vδ1 T cells was not affected in infants that had neonatal sepsis (Fig. S3, E and F).

In summary, spectral flow cytometric analyses revealed dynamic maturation patterns of Vγ9Vδ2 T cells after preterm birth mostly attributed to a decrease of CCR4, CD4 co-expression, and PD-1 expression, and an increased NK receptor expression, in infancy. Furthermore, no difference was found in the postnatal phenotypic maturation and surface protein expression of innate cytotoxic NK-related receptor frequencies between children with and without a diagnosis of sepsis in the neonatal period.

Single-cell transcriptome analysis identifies *HLA-DRA*^{hi} *CD83*$^{+}$ Vγ9Vδ2 T cells in neonatal sepsis

To decipher the underlying mechanisms of γδ T cell maturation characteristics and responsiveness in preterm infants during the first year of life and after neonatal sepsis, a combined single-cell transcriptome (scRNA-seq) and single-cell γδTCR sequencing (scTCR-seq) analysis was conducted. For this purpose, γδ T cells were isolated by flow cytometric sorting from peripheral blood samples of children with (n = 3) and without (n = 3) neonatal sepsis at the respective four time points after birth for NGS analysis (Table 2). Notably, neonatal sepsis was diagnosed in the three preterm infants on days 4, 27, or 29, respectively (Table 2). To further control for confounding factors influencing the transcriptional profiles, a pair of twins was included, where only one of the twins was diagnosed with sepsis (ID 20-040, Table 2). After quality control, a total of 33,771 γδ T cells from 15 NGS gene expression libraries generated from the six individual infants were considered for post-analysis. For technical reasons, namely the limited amount of blood lymphocytes collected at the first time point, the majority of γδ T cell transcriptomes were derived from peripheral blood samples from infants aged 1 mo, 6–8 mo, or 12–14 mo, as shown in Fig. S4, A and B. For the twin pair (ID 20-039 and 20-040), cord blood γδ T cells were profiled and represented γδ T cell transcriptomes before sepsis. For analysis, unsupervised clustering of all 33,771 γδ T cells with adjustment for differential gene expression analysis between clusters and uniform manifold approximation and projection (UMAP) identified nine clusters (c1–c9). The clusters c1–c9 were mapped to sepsis and sepsis-free infants, which were further divided by age of sampling into the sepsis period (1 mo of life) and the sepsis-free period (above 6 mo of age) (Fig. 4 A). The heat map of the top 100 differentially expressed genes (DEGs) between clusters represents the defined gene expression profiles of each cluster (Fig. 4 B and Fig. S4 C). Mapping of TRD and TRG clones by common cellular barcodes of scRNA-seq and scTCR-seq datasets to the identified nine clusters (c1–c9) defined Vδ1 T cells (mainly *TRDV1*, c1 and c2), Vγ9Vδ2 T cells (*TRGV9–TRDV2*, c4–c7), or a mixture of all *TRDV* sequences, with the majority being *TRGV9–TRDV2* (c3 and c8–c9) (Fig. 4 C and Fig. S4 D).

Next, to place the NGS in the context of other previously published single-cell transcriptome datasets, the clusters were annotated according to the top 50 DEGs and known gene expression profiles associated with naïve and effector γδ T cell profiles (Fig. 4 B) (Perriman et al., 2023; Sanchez et al., 2022; Tan et al., 2021). The Vδ1 T cell clusters (c1, c2) presented a predominantly naïve transcriptome, encoding for genes such as *LEF1*, *TCF7*, *NT5E* (encoding CD73) (Coffey et al., 2014), *CD27*, *SELL*, and *SOX4*, key regulators of immature T cells (McMurray et al., 2022; Sagar et al., 2020). In addition, the naïve Vδ1 T cells of clusters c1 and c2 were characterized by the expression of recent thymic emigration (RTE) markers: *KLF2*, *CCR9*, and *PECAM1* (encoding CD31) (Fig. 4 B) (Odumade et al., 2010; Sagar et al., 2020). These RTE-related transcripts increased at 6 mo of age (Fig. S4 E). In addition, calculation of single-cell gene signature module score for RTE per Vδ1 or Vδ2 T cells shows that the increase in RTE at 6 mo of age was predominately of Vδ1 T cells (Fig. 4 D), consistent with the two layers of fetal- and postnatal-derived TRD repertoires observed during infancy (Fig. S2). Notably, these transcripts were not reported in adult scRNA-seq data sets (Pizzolato et al., 2019; Tan et al., 2021), as they might be generally present in infancy by representing a postnatal thymic γδ (Vδ1) T cell wave (Fig. 4 E). Mapping the *TRDJ* gene element usage per cluster to identify postnatal- or fetal-derived γδ T cells, which are described to preferentially use *TRDJ1* or *TRDJ3* gene elements respectively (Papadopoulou et al., 2019), further confirmed the postnatal origin of clusters c1 and c2. In contrast, clusters c3–c6 were composed of fetal-derived cells with 60–65% of the clones arranged using *TRDJ3*, whereas clusters c7 and c8 were evenly distributed (Fig. S4 F).

Cluster c3 included the type 2 immunity–related genes *CD40LG*, *CCR4*, *CD4*, *IL4R* (Sanchez Sanchez et al., 2022; Tan et al., 2021), while cluster c4 included gene signatures related to type 3 immunity (e.g., *CCR6*, *RORC*, *BLK*, *S100A4*, *S100A6*) (Tan et al., 2021), although no *IL17A* or *IL17F* expression was detected (Fig. 4 B). Clusters c5–c7 consisted of innate cytotoxic Vγ9Vδ2 T cells as defined by the expression of *KLRB1* (encoding CD161) and the expression of cytotoxic-related genes and NK-related

Table 2. **Demographic and clinical characteristics of specific participants**

Participant	Gestational age (wk)	Birth weight (g)	Mode of delivery	Sex	Age at sampling (days)	Age at diagnosis of sepsis (days)	Blood culture (agent, age in days)
ID 21-018[a]	24.6	790	Caesarean section	Male	7, 33, 302, 518	29	*S. capitis*, 30
ID 21-019[a]	24.6	825	Caesarean section	Female	7, 33, 302, 518	4	*B. cereus*, 5
ID 20–040[b]	30.2	1,150	Caesarean section	Male	29, 267, 475	27	*S. marcescens*, 27
ID 20–039[b]	30.2	1,350	Caesarean section	Female	29, 267, 475	NA	–
ID 19–041	26.2	795	Caesarean section	Female	8, 26, 288, 465	NA	–
ID 19–042	31.3	1,920	Caesarean section	Female	5, 31, 244	NA	–

[a]Twin pair 1.
[b]Twin pair 2.

genes (e.g., *GZMA*, *GZMB*, *GNLY*, *KLRC1* (encoding for NKG2A), *KLRK1* (encoding NKG2D), *KLRD1* (encoding CD94), *NKG7*, *KLRG1*) (Pizzolato et al., 2019). The *IFNG* transcript was found preferentially in cluster c7. *IFNG* and *TNF*-type 1 transcripts were predominantly found in cluster *c7* and c8 of the Vγ9Vδ2 T cell subset. Finally, an unexpected cluster (c9) of *HLA-DRA*$^+$ γδ T cells expressing *CD69*, *CCR7*, *CD83*, and *CD74*, but no expression of cytotoxic related transcripts (e.g., *GZMA*, *GZMB*, *GNLY*), was identified and annotated as HLA-DR^{hi} CD83$^+$ γδ T cell cluster (Fig. 4 B). It was predominantly, but not exclusively, composed of Vγ9Vδ2$^+$ TCR cell clones (Fig. 4 C). Finally, when grouping the single-cell transcriptomes into sepsis versus no sepsis samples at the defined time points after birth, the HLA-DR^{hi} CD83$^+$ γδ T cell cluster c9 and IFN-γ cluster c8 were specifically abundant in neonates with sepsis (Fig. 4 E). All other clusters were equally present in neonates with and without sepsis (Fig. 4 E).

In conclusion, combined scRNAseq and scTCRseq of γδ T cells defined the transcriptional profiles of naïve and effector γδ T cell subsets in the first year of life in preterm infants diagnosed with and without neonatal sepsis and identified a subset of *HLA-DRA*, *CD83*-positive γδ T cells, which are enriched in sepsis and decreased during infancy.

Neonatal, but not adult blood, HMBPP-expanded Vγ9Vδ2 T cells become CD83$^+$

CD83 has been described on several immune cells known to inhibit or regulate T cell responses, such as Tregs and myeloid-derived suppressor cells (Grosche et al., 2020), but was rarely identified on γδ T cells (Howard et al., 2017; Tyler et al., 2017).

Additional analysis of single-cell gene expression profiles in Fig. 4, describing nine clusters (c1–c9) in relation to neonatal sepsis, confirms the higher expression of *CD83* in cluster c9 in sepsis and depicts higher gene expression of the early activation marker *CD69* in sepsis samples within clusters c5, c6, and c9 (Fig. 5 A). Violin plots further illustrate the higher expression of cluster c9–related genes such as *HLA-DRA*, *HLA-DRB1*, *CD83*, *CD74*, and *CD69* in infants with sepsis (Fig. 5 B). Thus, we aimed to validate the identified transcripts of cluster c9, namely *HLA-DR* and *CD83*, which had overall elevated expression in neonates during sepsis employing in vivo and in vitro approaches.

First, the frequency of CD83 on γδ T cells was measured by flow cytometry in an independent study population of preterm and term neonates aged 0–4 days. The neonates were divided into preterm and term neonates, with or without sepsis. The expression of CD83 on γδ T cells was donor dependent, with only a statistical difference in frequency among septic and uninfected term neonates (Fig. 5 C). Notably, peripheral blood was collected during the first 2 days of sepsis diagnosis, which may explain the inter-individual differences and lower abundance of CD83 surface expression in vivo as compared with the cluster c9 abundance in Fig. 4, which was mainly derived from 1-mo-old infants. Next, term cord blood mononuclear cells (CBMC) and preterm neonatal peripheral blood mononuclear cells (PBMC) were activated with microbial-derived HMBPP, which is known to be sensed by the Vγ9Vδ2$^+$ TCR and to induce Vγ9Vδ2 T cell expansion, or left untreated (IL-2 condition) for 7 days. To further compare age-dependent CD83 expression, samples from independent adult PBMC donors were included. Regardless of age and prematurity, HLA-DRA protein expression was increased after HMBPP stimulation (Fig. 5 D). Importantly, surface expression of CD83 was exclusively observed on preterm neonatal and term cord blood Vγ9Vδ2 T cells, and <10% of adult Vγ9Vδ2 T cells upregulated the CD83 receptor after TCR activation with HMBPP (Fig. 5 D). Consistent with the single-cell transcriptome analysis (Fig. 5 B), CD86 protein expression was low in stimulated neonatal and cord blood Vγ9Vδ2 T cells (Fig. 5 D). In contrast, the CD86 receptor was upregulated on expanded adult blood Vγ9Vδ2 T cells (Fig. 5 D). The differential protein expression of CD83 and CD86 by cord blood and adult blood Vγ9Vδ2 T cells was consistent at different HMBPP concentrations, with CD83 expression more evident on cord blood Vγ9Vδ2 T cells even at the lower HMBPP concentrations (Fig. S5 A). In conclusion, HMBPP-expanded neonatal Vγ9Vδ2 T cells from term and preterm neonates can express CD83 on their

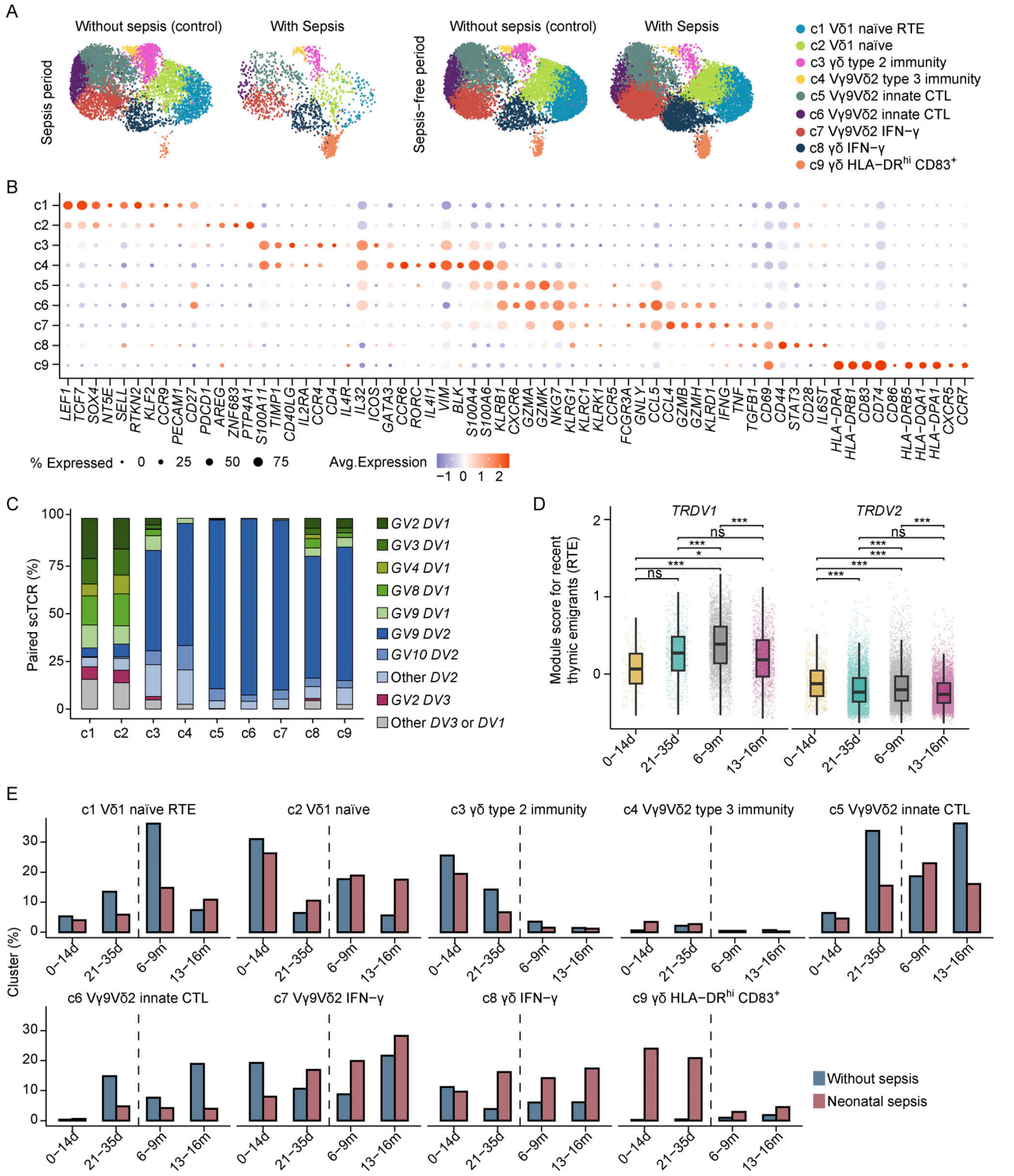

Figure 4. **Identification of *HLA-DRA*^{hi} and *CD83*$^{+}$ single-cell transcripts in preterm infants with sepsis.** Single-cell libraries were generated from peripheral blood γδ T cells of infants with (n = 3) and without (n = 3) neonatal sepsis sorted at different time points during the first year of life. **(A)** UMAP visualization of the γδ T cell scRNA-seq dataset from the infants with and without neonatal sepsis in the sepsis period (below 1 mo of age) and sepsis-free period (older than 6 mo) color-coded by clusters (c1–c9). **(B)** Dot plot of the average gene expression (columns) per cluster (rows), sized by the percentage of cells per cluster that expressed the respective gene (% Expressed). **(C)** Bar plots of the frequency of paired γδTCR V-gene usage compositions (*TRGV* and *TRDV*) in each cluster. Cells without a paired γδTCR were excluded. **(D)** Box plots of the single-cell gene signature module score for RTE at the indicated time points according to the *TRDV* gene usage. The RTE module score was computed based on *KLF2*, *CCR9*, *PECAM1*, *S1PR1*, *LEF1*, *TCF7*, *SOX4*, *NT5E*, and *SELL* genes. **(E)** Bar plots of the frequency of each cluster (c1–c9) at 0–14 days (d), 21–35 days, 6–9 mo (m), or 13–16 mo after preterm birth in children with and without neonatal sepsis (control). P values were determined by linear mixed effect modeling with multiple comparisons by Tukey (D); *P < 0.05, ***P < 0.001.

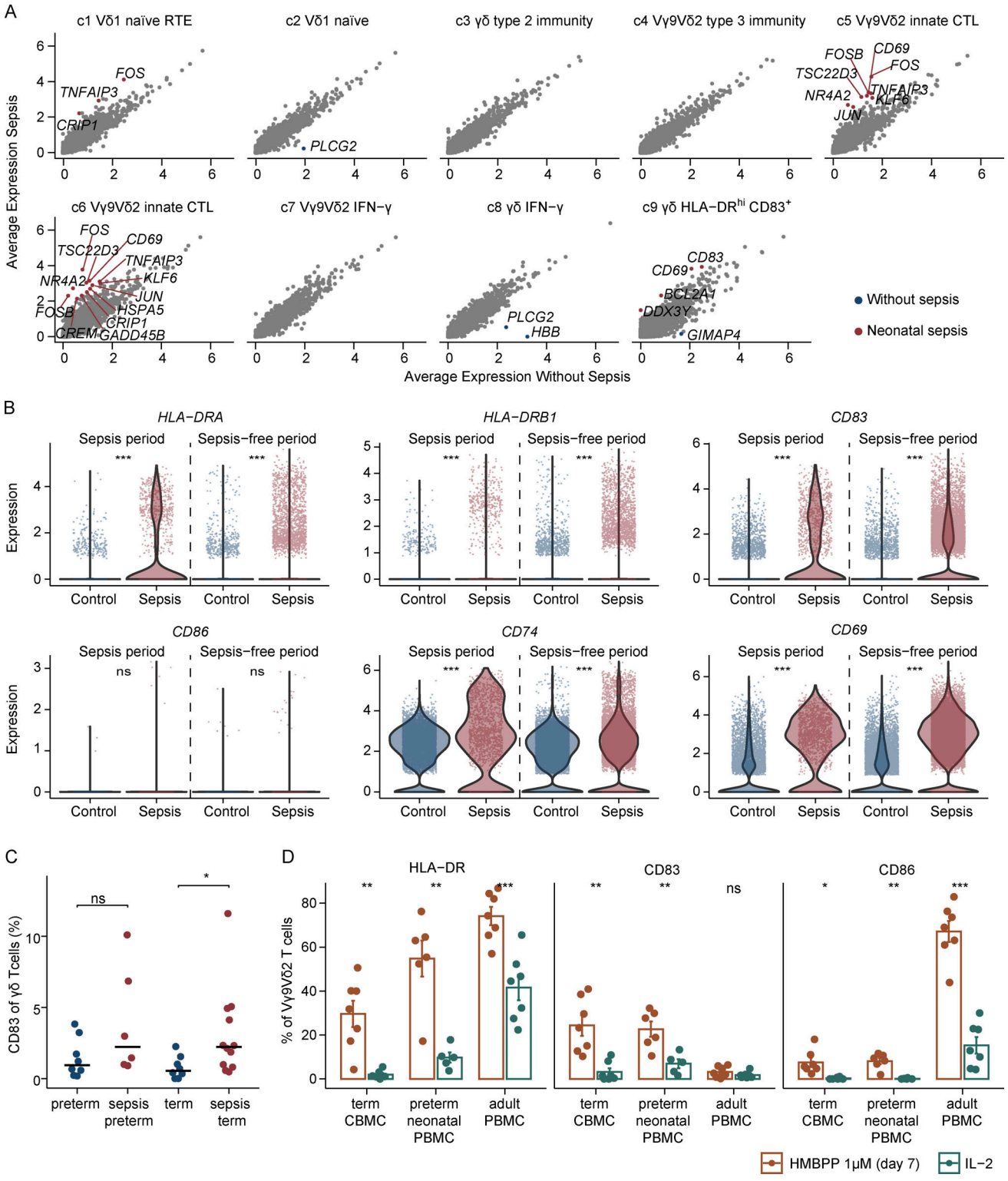

Figure 5. **Neonatal, but not adult blood, HMBPP-expanded Vγ9Vδ2 T cells become CD83⁺. (A)** Scatter plots of the average expression between conditions of the gene profiles in each of the annotated clusters, highlighting the genes that are more expressed in sepsis (pink) or without sepsis (blue). **(B)** Gene expression of *HLA-DRA*, *HLA-DRB1*, *CD83*, *CD86*, *CD74*, and *CD69* of γδ T cells from the children with and without neonatal sepsis in the sepsis period (<1 mo) and sepsis-free (>6 mo) period. **(C)** Frequency of CD83 on γδ T cells by flow cytometry in preterm or term neonates with sepsis (pink) during the first 2 days of diagnosis compared to age-matched uninfected controls (blue). **(D)** Frequency of HLA-DRA⁺, CD83⁺, and CD86⁺ cells of Vγ9Vδ2 T cells from term CBMCs (n = 7), preterm neonatal PBMCs (n = 6), and adult PBMC (n = 7) after 7 days of HMBPP (red) or IL-2 only (green) measured by flow cytometry in four independent experiments. Bar plots represent the mean ± standard error. P values were determined by Mann–Whitney U (B and C) or paired t test (D); ns = not significant, *P < 0.05, **P < 0.01, ***P < 0.001.

surface, and this was a unique feature of neonatal and cord blood Vγ9Vδ2 T cells.

HMBPP-expanded Vγ9Vδ2 T cells from neonatal blood do not induce CD4 T cell proliferation

To better define a potential function of the sepsis-induced cluster c9, a gene ontology (GO) enrichment analysis of upregulated DEGs from the respective clusters c1–c9 was performed. This analysis revealed the enrichment of GO terms related to antigen processing and cell trafficking for cluster c9 (Fig. S5 B). This was consistent with the identified upregulated genes of cluster c9, including *HLA-DRA*, *HLA-DRB1*, *HLA-DRB5*, *CD74*, *CD69*, and *CXCR5*, as shown in the volcano plot (Fig. S5 C). Antigen-processing capabilities and interaction with conventional αβ T cells were previously demonstrated for activated adult Vγ9Vδ2 T cells, which express HLA-DR and various coreceptors, including CD86 (Brandes et al., 2005; Howard et al., 2017). However, in contrast to known surface molecules of adult γδ T cells with antigen-presenting capabilities (Barisa et al., 2017; Brandes et al., 2005; Holmen Olofsson et al., 2021; Tyler et al., 2017) or professional antigen-presenting cells, CD83 but not CD86, was expressed on HMBPP-expanded neonatal γδ T cells (Fig. 5). Also the sepsis-induced cluster c9 showed *CD83*, but not *CD86* expression (Fig. 5). Therefore, we next evaluated the antigen processing capacity of Vγ9Vδ2 T cells described in adults (Meuter et al., 2010) and how this compares to neonatal γδ T cells. For this purpose, a DQ ovalbumin (DQ-OVA) assay on HMBPP-expanded Vγ9Vδ2 T cells from term CBMCs, neonatal, and adult PBMCs was performed. Vγ9Vδ2 T cells from HMBPP-stimulated adult and neonatal PBMCs efficiently captured and degraded the DQ-OVA, whereas Vγ9Vδ2 T cells from HMBPP-stimulated CBMC appeared to be less efficient in this process (Fig. 6, A and B). Next, the ability of term cord blood, preterm neonatal, and adult blood Vγ9Vδ2 T cells to induce CD4 αβ T cell proliferation and activation was tested using a mixed lymphocyte reaction (MLR) system. To this end, Vγ9Vδ2 T cells (stimulators) were sorted by flow cytometry from CBMCs, neonatal and adult PBMCs after 7 days of HMBPP expansion, and subsequently cocultured with allogeneic CD4 αβ T cells (responders), prior to depletion of γδ T cells and the regulatory T cells ($CD25^{hi}$/$CD127^{lo}$) within the CD4 αβ T cells. After 6 days of coculture, CD4 T cell responder cells proliferated in the presence of inactivated adult blood Vγ9Vδ2 T cells but not cord blood and neonatal blood Vγ9Vδ2 T cells (Fig. 6, C and D). In addition, adult but not neonatal blood Vγ9Vδ2 T cells induced CD4 αβ T cell activation as measured by upregulation of CD25, HLA-DRA, PD1, and CTLA-4 (Fig. 6 E). In conclusion, these experiments suggested that adult, but not neonatal, Vγ9Vδ2 T cells can interact with CD4 αβ T cells in an αβTCR:MHC-II and CD28:B7-dependent manner (Greenwald et al., 2005), mostly attributed to an age-dependent acquisition of CD86 versus CD83 upon activation with the microbial-derived metabolite HMBPP, respectively.

Discussion

Early in life, the human immune system senses a series of environmental cues. Systems immunology approaches have advanced our understanding of global signatures of immune cell maturation signatures across the human lifespan, with further evidence of stereotypic immune cell development in early life (Brodin et al., 2015; Olin et al., 2018). However, information on individual cell populations, particularly those that are generated in the fetal period including γδ T cells, is sparse (De Rosa et al., 2004; Papadopoulou et al., 2020; Parker et al., 1990; Ravens et al., 2020; van der Heiden et al., 2020). By monitoring γδ T cells and their TCR repertoires in a longitudinal cohort of preterm neonates, this study provided a reliable reference map of the abundance and phenotypic composition of Vγ9Vδ2 and Vδ1 T cells after preterm birth. Specifically, TCR repertoire analysis revealed a shift in clonal composition from fetal-derived T cell clones with low N-insertions present at the beginning of life to a more diverse repertoire at 6 mo, which was evident in each preterm infant. These TRD repertoire patterns are thought to be caused by an age-dependent increase in terminal deoxynucleotidyl transferase enzyme expression in thymocytes (Davenport et al., 2020; Deibel et al., 1983) and pre- and postnatal thymic output of the different γδ T cell subsets (Papadopoulou et al., 2019; Perriman et al., 2023; Sanchez et al., 2023). Notably, further systematic analysis showed that fetal clones persisted at similar low frequencies in both preterm and term infants at 1 year of age. In addition, phenotypic and transcriptional analyses revealed different postnatal maturation characteristics of Vγ9Vδ2 versus Vδ1 T cells in preterm infants. While Vδ1 T cells were predominantly naïve at birth and underwent only minor phenotypic changes within the first year of life in our cohort of preterm neonates, Vγ9Vδ2 T cell maturation characteristics were dynamic. In particular, the first weeks of life were associated with a type 2 immune phenotype and the expression of checkpoint molecules such as PD-1. The latter is thought to be one molecule important for tolerating the sum of new environmental cues in the neonatal period (Hsu et al., 2016). Later in infancy, Vγ9Vδ2 T cells acquired NKG2A expression, which is associated with a type 1 immune phenotype in infants (Hsu et al., 2021). Taken together, and as suggested for other immune system parameters (Olin et al., 2018), the postnatal age and age-related factors common to all neonates appear to drive the postnatal adaptation of γδ T cells.

Specifically, the Vγ9 T cell subsets represented, on average, 4–5% of the T cell pool in the peripheral blood of 1-mo-old preterm neonates. It may therefore represent an important set of innate T cells in neonates (Gibbons et al., 2009; Papadopoulou et al., 2020; Rahman Qazi et al., 2021). The data show that the increased frequencies of Vγ9Vδ2 T cells within the first weeks of life were independent of factors that might alter the microbial composition, such as the mode of delivery and antibiotics treatment. Only a severe immunological perturbation, neonatal sepsis, affected and enhanced the initial postnatal increase of Vγ9Vδ2 T cells. In addition, TCR repertoire analyses showed that specifically Vγ9Vδ2 T cells derived from early fetal thymic development were the dominant source of Vγ9Vδ2 T cells in this time window and further expanded in neonatal sepsis, either by higher responsiveness or predominance of this subset during this period of life, which is independent of prematurity.

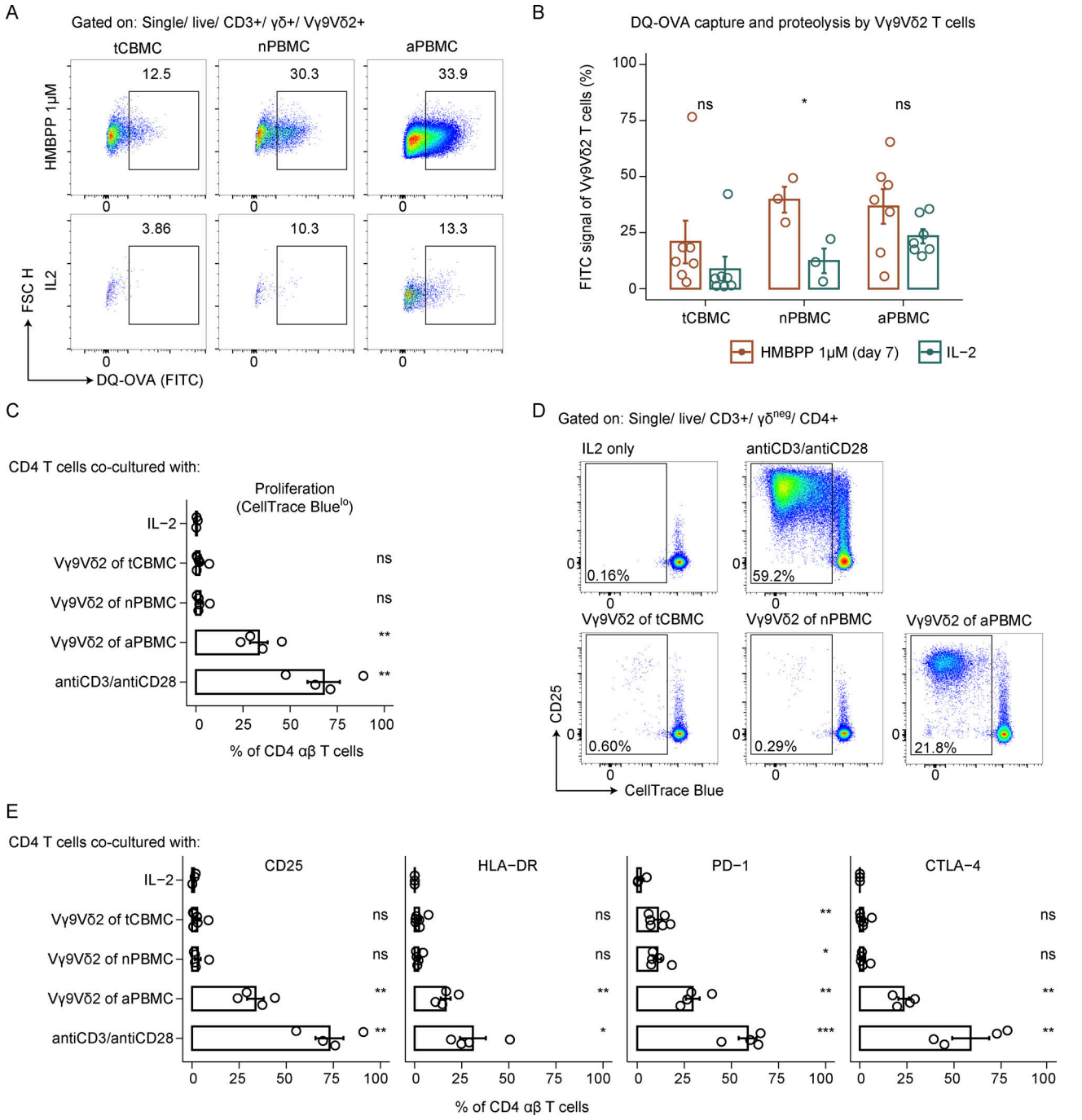

Figure 6. **HMBPP-expanded Vγ9Vδ2 T cells from neonatal blood do not induce proliferation of CD4 T cells. (A)** Representative dot plots showing the DQ-OVA signal (FITC) on Vγ9Vδ2 T cells from one term cord blood (tCBMC), one neonatal blood donor (nPBMC) and one adult blood donor (aPBMC) after 7 days with IL-2 or HMBPP stimulation. **(B)** Frequency of DQ-OVA signal (FITC) on HMBPP-expanded Vγ9Vδ2 T cells from term CBMCs (tCBMC, *n* = 7), neonatal PBMCs (nPBMC, *n* = 3), and adult aPBMC (*n* = 7) after 7 days of HMBPP (red) or IL-2 only (green) measured by flow cytometry in three independent experiments. **(C–E)** Vγ9Vδ2 T cells were isolated from term CBMC (tCBMC), neonatal PBMC (nPBMC), and adult PBMC (aPBMC) after 7 days of HMBPP stimulation, and cocultured after irradiation with allogenic sorted CD4 T cells ($CD4^+/\gamma\delta^{neg}/CD25^{lo}/CD127^+$). Flow cytometry analysis was performed after 6 days of coculture. Proliferation of CD4 T cells was determined by CellTrace Blue dilution. Data were generated in two independent experiments. **(C)** Frequency of CellTrace $Blue^{lo}$ (proliferating) CD4 T cells after 6 days of co-culture with the indicated conditions. **(D)** Representative dot plots showing the CellTrace Blue dilution and CD25 expression of CD4 T cells of one adult donor in the presence of allogenic irradiated Vγ9Vδ2 T cells from one tCBMC, one nPBMC, and one aPBMC sample in comparison to IL-2 unstimulated control and antiCD3/antiCD28 control. **(E)** Frequency of CD25, CTLA-4 (intracellular), PD1, and HLA-DRA surface marker expression of CD4 T cells after 6 days of co-culture with the indicated conditions. P values were determined by paired *t* test using IL-2 condition as the reference (B, C, and E); ns = not significant, *P < 0.05, **P < 0.01, ***P < 0.001.

The Vγ9Vδ2⁺ TCR responds to small metabolic compounds, called phosphoantigens, through the interaction with BTN3A1 and BTN2A1 ligands (Herrmann and Karunakaran, 2022; Morita et al., 2007). These can be either self or pathogen-derived (Morita et al., 2007). In particular, HMBPP is produced by most Gram-negative bacteria, but not by the clinically relevant Gram-positive bacteria (e.g., *Staphylococcus* spp., *Streptococcus* spp., and *Enterococcus* spp.) (Eberl and Moser, 2009) and has been shown to induce innate-like polyclonal expansion and activation of cord blood and adult blood Vγ9Vδ2 T cells (Fichtner et al., 2020a). Future studies are needed to investigate how the Vγ9Vδ2 TCR itself and together with secondary signals ensure optimal and balanced microbiota-induced immune cell activation under homeostatic conditions in neonates and retain the potential to recognize pathologic condition, namely bacterial-induced sepsis, resulting in an acute Vγ9Vδ2 T cell expansion.

To date, Vγ9Vδ2 T cell functionalities in utero and neonates have been primarily associated with granzyme and interferon production (Sanchez Sanchez et al., 2023). Surprisingly, single-cell transcriptome analyses additionally identified a specific Vγ9Vδ2 T cell cluster in children with sepsis, enriched for *CD83*, *HLA-DR*, and other genes related to antigen presentation, with no expression of type 1 immunity genes. The fact that the sepsis-induced cluster had a lower abundance in 6-mo and 1-year-old neonates after sepsis suggests that sepsis is not the main driver of postnatal maturation and does not perturb γδ T cell profiles in infancy, which might be in contrast to other T cells (Yang et al., 2022). In addition, a Vγ9Vδ2 T cell cluster associated with *IFNY* transcripts was found to be more abundant in infants with sepsis during and after the infection, showing an additional functional capability of this innate T cell subset in early life in response to systemic infections.

Studies using in vitro stimulation assays provided evidence for antigen processing capabilities and interaction with conventional CD4 or CD8 T cells of Vγ9Vδ2 T cells in adults (Barisa et al., 2017; Brandes et al., 2005; Holmen Olofsson et al., 2021; Tyler et al., 2017), consistent with what was observed here in Vγ9Vδ2 T cells from adult blood. Regardless of age, Vγ9Vδ2 T cells were able to take up and proteolytically degrade proteins. This might be further linked to the expressed genes (e.g., invariant chain CD74 important for assembly of the MHC II complex) (Dijkstra and Yamaguchi, 2019) in the neonatal sepsis cluster c9. Thus, one could speculate that γδ T cells may compensate for the less mature professional antigen-presenting cells in neonates and functionally adapt in these circumstances (Olin et al., 2018). A similar concept has been proposed in adult malaria-infected individuals (Howard et al., 2017). However, there is a caveat: only adult Vγ9Vδ2 T cells, but not cord and neonatal blood Vγ9Vδ2 T cells, induced CD4 T cell proliferation in the MLRs performed here, clearly indicating a different biology of neonatal and adult γδ T cells.

The answer to one function of γδ T cells in sepsis may come from transcriptome analyses, which indicate high levels of *CD83* gene expression in the neonatal sepsis–enriched γδ T cell cluster. Further in vitro assays demonstrated that the CD83 acquisition is induced by bacterial-derived HMBPP and predominantly expressed by cord blood and neonatal blood Vγ9Vδ2 T cells after stimulation. The expression of CD83 on activated Vγ9Vδ2 T cells has been previously detected in adults, but with an early and transient surface expression, when the Vγ9Vδ2 expansion has not occurred (Howard et al., 2017). On the contrary, adult Vγ9Vδ2 T cells have a more stable expression of the costimulatory receptor CD86,[39] as also confirmed by us.

CD83 is present in a variety of immune cells, including regulatory T cells, dendritic cells, and myeloid-derived suppressor cells, and is known to play an important role in orchestrating proper immune responses and inducing resolution of inflammation (Grosche et al., 2020). Similar to Vγ9Vδ2 T cells, myeloid-derived suppressor cells are present at high levels in neonates (Gervassi et al., 2014; He et al., 2018). In neonates, they suppress T cell responses and inflammation (Gervassi et al., 2014; He et al., 2018). The MLRs performed here revealed that HMBPP-expanded, activated cord blood and neonatal blood CD83⁺ Vγ9Vδ2 T cells do not induce proliferation of whole CD4 T cells, which may be in part caused by the absence of costimulation, as they lack CD86 expression, or by their capacity to release soluble CD83, which has been shown to inhibit allogeneic T cell proliferation (Lechmann et al., 2001). Therefore, we hypothesize an immune regulatory capacity of Vγ9Vδ2 T cells in neonatal sepsis. This idea may be further supported by the increased expression of PD-1 on Vγ9Vδ2 T cells in infancy observed by us and others (Hsu et al., 2016, 2021). Taken together, these results represent a new level of functional adaptability of γδ T cells in neonates and highlight fundamental differences between neonatal and adult blood γδ T cells.

Limitations of the study

Neonatal sepsis is characterized by an early dominant hyperinflammatory state and a transition to an anti-inflammatory immune state with sepsis-induced immunosuppression (Dowling and Levy, 2014). In this study, the transcriptomic profiles are mostly from late time points in the sepsis period, 3–5 days after the diagnosis of LOS, which may explain the heterogeneity of CD83 expression in the preterm and term neonates with early-onset sepsis, observed in the independent study population. In addition, it was technically difficult to perform transcriptome analysis on neonatal blood from 3–10-day-old newborns, which results in limited transcriptional profiles prior to sepsis. Furthermore, type 1 effector γδ T cells expand after birth (Papadopoulou et al., 2020), and this was consistent with an increase in CCR5⁺ Vγ9Vδ2 T cells during the first weeks of life in this study cohort (Glatzel et al., 2002). Therefore, we cannot exclude that granzyme-producing Vγ9Vδ2 T cells may additionally expand and have enhanced functionality with the onset of sepsis. Importantly, and supported by the in vitro analyses, our data suggest that Vγ9Vδ2 T cells may contribute to a shift toward immune regulatory capacities in sepsis-induced inflammation. Thereby, it will be important to further address the possibility of whether neonatal γδ T cells drive the polarization of naïve CD4 T cells toward a regulatory phenotype. Together, these findings indicate a higher phenotypic diversity of fetal-derived Vγ9Vδ2 T cells as previously anticipated, and this diversity may be important to

adapt to the required immunological needs in early life and inflammatory settings. A similar concept has recently emerged in the context of cancer in adults (Harmon et al., 2023; Reis et al., 2022). Finally, it remains to be seen whether Vγ9Vδ2 T cells respond and acquire this phenotype specifically in neonatal sepsis, or whether this is a general phenomenon applicable to any inflammation and/or age group.

Materials and methods

Study populations and PBMC isolation

PBMCs were freshly isolated by Ficoll–Paque density gradient centrifugation from blood samples collected from a longitudinal cohort of 100 preterm infants at four time points, namely 1–14 days, 21–35 days, 6–10 mo, and 13–19 mo after birth (Table 1) (Marißen et al., 2019). A median of 785 µl (range 360–1,750) of EDTA blood was collected at 1–14 days of age, 830 µl (range 550–1,900) at 21–35 days of age, 1,300 µl (range 550–2,970) at the 6–10 mo of age or 1,675 µl (range 850–3,000) at the 13–19 mo of age. For 73 newborns, heparin blood was collected from cord blood with a median of 17 ml (range 0.55–82.5). After isolation, mononuclear cells were frozen in 90% fetal bovine serum (FBS) (Sigma-Aldrich) and 10% DMSO (Sigma-Aldrich) freezing medium and stored at −80°C until use. Sample series collected at more than three time points were obtained from 71 (71%) preterm infants. The neonates were born at the median gestational age of 30.4 wk (range, 23.1–32.5) based on the last menstrual period. The degree of prematurity was categorized according to the World Health Organization definitions as either extreme (<28 wk of gestational age, n = 25), very (28.1–32 wk, n = 57), or moderate (32.1–34 wk, n = 18). In 76% of the cases, the infants were delivered by caesarean section; 52% of the preterms were from a singleton pregnancy. The infants of this study had various clinical conditions associated with preterm birth, with a median length of hospital stay after birth of 51 days (range 21–190), and diverse environmental exposures afterward (Table 1). The preterms received formula plus breast milk within the first months of life, while introduction of solid food was started at around 6 mo of life.

In addition, EDTA blood was collected for in vitro assays from 3- to 6-wk-old uninfected preterm infants (n = 9) born by caesarean section at a median gestational age of 29 wk (range 24–31) with a median birth weight of 1,210 g (695–1,485) at the AUF DER BULT Children's and Youth Hospital, Hannover, Germany. From the same hospital, 100–750 µl EDTA blood was collected for FACS analysis from 0- to 4-day-old uninfected neonates (n = 8 preterm, n = 8 term) and 0- to 4-day-old neonates with sepsis (n = 6 preterm, n = 12 term). CBMCs (n = 10) were collected from uncomplicated, full-term pregnancies delivered at the Hannover Medical School. Peripheral blood from healthy adult controls was collected from healthy volunteers (n = 11) at the Department of Transfusion Medicine at the Hannover Medical School.

Ethical approval

The recruitment of the participants and sample collection were conducted according to the principles expressed in the Declaration of Helsinki and approved by the Institutional Review Board of the Hannover Medical School (no. 6031-2011, no. 6031-2015, no. 8014_BO_S_2018, no. 1303-2012, no. 10856_BO_K_2023 [the latter was approved in collaboration with the Children's and Youth Hospital AUF DER BULT]). Before sample collection and enrolment to the study, written informed consent was obtained from all donors (parents or guardians in the case of cord blood and children).

Definitions

Neonatal sepsis

Neonatal sepsis was defined following the criteria of the national infection surveillance system "NEO-KISS." Clinical sepsis and microbiologically confirmed sepsis were included as neonatal sepsis. Clinical sepsis was diagnosed in the presence of at least two of the following criteria: temperature >38°C or <36.5°C, tachycardia >200/min, occurrence or increase of hypoxemia, bradycardia or apnea, hemodynamic instability, hyperglycemia >10 mmol/liter, metabolic acidosis, grayish skin color, and prolonged reperfusion time, or one clinical and at least one laboratory sign (C-reactive protein >20 mg/liter, IL-6 >300 ng/liter, a ratio of immature to total neutrophils of >0.2, white blood cell count <5/nl, and platelet count <100/nl), and antibiotic treatment for a minimum of 5 days, if no proof of causative agent in the blood culture. Microbiologically confirmed sepsis presented clinical signs of sepsis with pathogen growth in the blood culture.

Sepsis period

The sepsis period was defined when the blood sample was collected at the time of sepsis diagnosis and up to 28 days after the initial diagnosis. More than 2 mo after the initial diagnosis was considered sepsis-free period.

Antibiotics prebirth

Antibiotics prebirth was defined as positive when the mother received antibiotics 48 h before birth.

AIS

AIS was defined as maternal fever (≥38°C) and at least two of the following clinical or laboratory signs: maternal leukocytosis (>15,000 cells/µl), maternal tachycardia (>100 bpm), fetal tachycardia (>160 bpm), uterine tenderness, or foul smell of amniotic fluid, while another maternal infection site had been excluded.

Postnatal steroids

Postnatal steroids were considered when the infant received at least one cycle of parenteral steroids in the first month of life.

Spectral flow cytometry analysis

For spectral flow cytometric analysis, frozen mononuclear cells were thawed, washed in phosphate-buffered saline (PBS), and incubated with the listed antibodies (Table S2) for 20 min at room temperature. After washing off excess antibodies, cells were acquired on an Aurora spectral flow cytometer (Cytek). Spectral flow cytometry data were acquired using SpectroFlo version 2.2.0 (Cytek) and analyzed with FCS Express 7 (Denovo).

The PCA was computed using the R package factoextra on R version 3.12. For the study population of preterm and term neonates in Fig. 5 C, total PBMC were stained with fixable viability dye (Zombie NIR; BioLegend), anti-CD3 Alexa Fluor 532 (clone UCHT1; BD Bioscience), anti-γδ TCR PE-Vio770 or APC (clone REA591; Miltenyi Biotec), and anti-CD83 Pe-Cy5 (clone HB15e; BioLegend).

Flow cytometric sorting and bulk TCR-seq analysis

Bulk TRG and TRD repertoires of 33 participants were generated from FACS-sorted γδ T cells from fresh or frozen PBMC at the respective time points: 1–14 days (n = 13), 21–35 days of age (n = 27), 6–9 mo (n = 25), and 13–16 mo of age (n = 14). For 25 neonates, the available TRG and TRD repertoires and the generated FACS data of the first two time points, namely 1–14 days (n = 13) and 21–35 days of age (n = 18) were taken from our previous study (BioProject PRJNA592548) (Ravens et al., 2020). Furthermore, for the present study, data of additional later time points of these 25 neonates were generated and included in the analyses, namely 6–9 mo (n = 19) and 13–16 mo of age (n = 9). TRD repertoires for five-term infants were taken from BioProject PRJNA592548 (Ravens et al., 2020). For all samples of the 58 preterm neonates, PBMCs were stained for 20 min for flow cytometric analysis and cell sorting. Dead cells were detected via DAPI staining. The following antibodies were used: anti-CD3 PE-Cy7 (clone SK7; BD Bioscience), anti-γδ TCR PE or APC (clone REA591; Miltenyi Biotec), anti-Vγ9 FITC (clone REA470; Beckman Coulter), anti-Vδ1 (clone REA173; Miltenyi Biotec), anti-CD19 BV605 (clone SJ25C1; BD Bioscience), anti-CD20 PE (clone 2H7; BioLegend), anti-CD8 APC-Cy7 (ECK1; BioLegend), anti-CD4 PerCP (M-T466; Miltenyi Biotec), anti-CD16 BV785 (3G8; BioLegend), anti-CD27 Alexa Flour 700 (clone O323; BioLegend), anti-CD38 BV711 (HIT2; BioLegend), anti-CD5 PerCPCy5.5 (L17F12; BioLegend), and anti-IgD BV510 (IA6-2; BD Bioscience). Dead cells were detected via DAPI staining. Samples were sorted for single/live/CD3/γδ T cells on a FACS Aria or FACS Fusion Cell Sorter (BD Bioscience). Generated FACS data of cell sorting were analyzed with Flowjo 10.0 software. For the following TRG and TRD repertoire analyses, RNA isolation (Qiagen) and cDNA synthesis (SuperScript III; Invitrogen) were performed after cell lysis in RLT lysis buffer (Qiagen). Next, CDR3 regions of the TRG or TRD were amplified via gene-specific primers as previously described (Ravens et al., 2017, 2020). Libraries were sequenced (paired-end, 500 cycles) on the Illumina MiSeq platform. Demultiplexed read 1 files were processed for downstream analysis. The fastq files were annotated according to the International Immunogenetics Information System (IMGT) using MiXCR software (Bolotin et al., 2015). Annotated read files were summarized and analyzed using VDJTools (Shugay et al., 2015) and R version 3.12. Simpson diversity indices were calculated with the R library immunarch. Treemaps were plotted using the R package Treemap. Clustering analysis of the TRD repertoire from 58 preterm neonates at four time points and five-term infants aged 12–24 mo was performed using the KAy-means for MIxed LArge data (KAMILA) clustering algorithm (Foss et al., 2016) implemented in the R kamila package, with the following input variables: *TRDV*, *TRDD*, and *TRDJ* usage, as well as the CDR3 length, the introduction of random nucleotides (N additions) and the number of donors in which each unique CDR3aa clone was found (occurrences). The optimal number of clusters was determined using the recommended prediction strength method of Tibshirani and Walther (2005). The TCR clone publicity was assigned based on occurrence in private if the CDR3 sequence was present in only single individuals, public if it occurred in two to half of the individuals (<29), and shared public if the clone was present in more than half of the donors (≥29) in a total of 58 preterm children.

scRNA-seq and scTCR-seq libraries generation and processing

Thawed PBMC were incubated at 37°C for 1 h in an RPMI medium 1640 (Gibco) supplemented with 10% FBS (Sigma-Aldrich), 1% *L*-glutamine, 1 mM sodium pyruvate, and 1% streptomycin-penicillin (all Gibco), followed by antibody staining with anti-CD3 PE-Cy7 (clone SK7; BD Bioscience), anti-γδ TCR PE or PerCP-Vio700 (clone REA591; Miltenyi Biotec), anti-αβ FITC (clone WT31; BD Bioscience), and anti-CD19 BUV605 (clone SJ25C1; BD Bioscience). Dead cells were detected via DAPI staining. For the twins (ID 20-039 and ID 20-040), each time point was marked with the TotalSeq C0251, C0252, C0253, or C0254 anti-human hashtag antibody before sorting. The single/live/CD3/$\alpha\beta^{neg}$/γδ T cells were sorted on a FACSAria III Fusion (Becton-Dickinson). Libraries for scRNA-seq and scTCR-seq were prepared from 600 to 10,000 sorted γδ T cells mixed with 2,000–10,000 sorted B cells (for libraries of ID 21-018, ID 21-019, ID 20-039 and ID 20-040) using the Chromium Single-Cell 5′ Library Gel Bead, and Construction Kit and Chromium Single-Cell V(D)J Enrichment Kit (10x Genomics) according to the user guidelines. The single-cell TCR, gene expression, and surface libraries were generated according to the Chromium Single Cell V(D)J protocol (10x Genomics). Briefly, 100 µl of GEMs ("Gel bead in EMulsion" droplets) containing single-cell barcoded full-length cDNA were generated in Chromium Next GEM Chip G. After clean-up and cDNA amplification, the supernatant was used for the cell Surface Protein Library. Before fragmentation, 7 µl of GEMs were used to amplify γδ TCR sequences by using a custom primer targeting the *TRDC* and *TRGC* gene segments as described previously (Tan et al., 2021). The rest of the GEMs were then used for fragmentation and gene expression library construction according to 10x Genomics guidelines. Agilent Bioanalyzer High Sensitivity chips were applied for quality control of the libraries. The scRNA-seq and surface libraries were sequenced on the Illumina NextSeq 500/550 platform. The scTCR-seq libraries were sequenced on the Illumina MiSeq or the Illumina NextSeq 500/550 platform.

Sequence reads were aligned to reference the human genome GRCh38-3.0.0. The demultiplexing and the cell barcode-gene matrices were counted with Cell Ranger 3.1 (10x Genomics). The cell barcode-gene matrices were then processed with Seurat v4.0.1 under R v4.0.3 to remove low-quality cells (genes <200, features >3,000, % mitochondrial genes >25). Cells from ID 20-039 and ID 20-040 were demultiplexed for each time point based on the hashtag oligos enrichment. B cell depletion was performed by selecting cells without expression of CD19, CD20, or any of the immunoglobulin-heavy constant genes. Cell

scRNA-seq data were merged for further normalization, scaling, and dimensional reduction using Seurat functions. The batch effect was removed with the function "RunHarmony," a Seurat function applied from the Harmony package. Cells were clustered with "FindCluster" function and annotated according to the expression of specific genes (visualized with "DotPlot" function). The aggregated expression score for RTE was calculated with "AddModuleScore" function based on *KLF2*, *CCR9*, *PECAM1*, *S1PR1*, *LEF1*, *TCF7*, *SOX4*, *NT5E*, and *SELL* genes. DEG analysis between clusters was assessed with "FindMarkers" function for transcripts detected in at least 10% of cells using logFC (log-fold-change) threshold of 0.25. The GO (biological process) enrichment analysis was performed with the top 100 significant DEG by cluster, excluding the mitochondrial, ribosomal, and TCR genes, using the R package clusterProfiler. The differential expressed genes across conditions in each of the annotated clusters were considered when the difference in average gene expression was ±1.45 times between conditions.

HMBPP in vitro stimulation

Prior to culture, thawed adult PBMC and CBMC were rested in a humidified CO2-incubator at 37°C at a slant of 5° above horizontal for 18 h (Wang et al., 2016) in advanced RPMI medium (Gibco) supplemented with 10% heat-inactivated FBS (Sigma-Aldrich), 1% GlutaMAX, 50 µM β-mercaptoethanol, and 1% streptomycin-penicillin (all Gibco). Neonatal PBMC were isolated from fresh blood samples by Ficoll gradient centrifugation and immediately used for culture. The mononuclear cells were stimulated at a concentration of 2×10^6 cells/ml and a growth surface area of 0.5–0.6 cells/cm^2 with 1 µM HMBPP (unless otherwise indicated) and 100 U/ml IL-2 (Sigma-Aldrich) with or without 20 ng/ml IL-15 (Peprotech). After 72 h of culture, 100 IU/ml of IL-2 was added. On day 6 of culture, the media with 100 IU/ml was renewed for phenotyping assays and sorting of Vγ9Vδ2 T cells on day 7 of culture. Unstimulated cells were maintained in culture with 100 U/ml IL-2 for phenotyping assays.

DQ-OVA assay

The antigen-processing capacity of stimulated and unstimulated Vγ9Vδ2 T cells was determined on day 7 of HMBPP stimulation by incubating 5×10^5 cells per condition with 10 µg/ml DQ-OVA (Thermo Fisher Scientific) for 20 min at 37°C. After the initial incubation, cells were washed twice with cold growth medium and chased for an additional 100 min at 37°C. At the end of the chase period, cells were washed once with FACS buffer and analyzed by flow cytometry on a Cytek Aurora. Endocytosis and proteolysis of DQ-OVA by Vγ9Vδ2 T cells were measured as increasing fluorescence on the FITC channel (BODIPY FL fluorophore).

MLR

To test the induction of CD4 αβ T cells proliferation and activation by Vγ9Vδ2 T cells, MLR assays were performed. Vγ9Vδ2 T cells were used as stimulators and allogenic CD4 T cells as responders. For this CBMC, neonatal PBMC and adult PBMC were harvested after 7 days of HMBPP stimulation, washed, and incubated for 20 min at room temperature with fixable viability dye (Zombie Violet; BioLegend) and the following antibodies: anti-CD3 BV510 (clone UCHT1; BioLegend), anti-γδ TCR PE-Vio770 (clone REA591; Miltenyi Biotec), anti-Vγ9 APC (clone REA470; Miltenyi Biotec) and anti-Vδ2 APCVio770 (clone REA771; Miltenyi Biotec). The single/live/CD3/γδ TCR/Vγ9Vδ2 T cells were sorted to 97–99% purity and irradiated at 12 Gy prior to coculture with responder cells. For the responder cells, the non-CD4 T cells were depleted from allogeneic PBMC using the MojoSort Human CD4 T cell Isolation Kit (BioLegend). The untouched CD4 T cells were collected from the magnetic separator to 95–97% purity and incubated for 20 min at room temperature with fixable viability dye (Zombie Violet; BioLegend) and the following antibodies: anti-CD3 BV510 (clone UCHT1; BioLegend), anti-γδ TCR APC (clone REA591; Miltenyi Biotec), anti-CD127 (IL-7Rα) BV650 clone A019D5; BioLegend), anti-CD25 PE-Fire700 (clone M-A251; BioLegend), anti-CD45RA BV605 (clone HI100; BioLegend), and anti-CCR7 (CD197) APC-R700 (2-L1-A; BD Bioscience). The untouched CD4 T cells were depleted from the $\gamma\delta^+$ TCR and regulatory T cells ($CD25^{hi}/CD127^{lo}$) by FACS sorting to 96–99% purity. The FACS-sorted CD4 T cells were then labeled with CellTrace Blue for proliferation measurement. Next, the irradiated Vγ9Vδ2 T cells and sorted CD4 T cells were cocultured at a 1:10 ratio for 6 days. After this, the harvested cells were stained with the following antibodies: anti-CD3 BV510 (clone UCHT1; BioLegend), anti-CD4 BUV496 (clone RPA-T4; BD Bioscience), anti-γδ TCR PE-Vio770 (clone REA591; Miltenyi Biotec), anti-PD1 BUV737 (clone EH12.1; BD Bioscience), anti-HLA-DR BV570 (clone L243; BioLegend), anti-CD25 PE-Fire700 (clone M-A251; BioLegend), anti-CD45RA BV605 (clone HI100; BioLegend), anti-CCR7 APC-R700 (clone 2-L1-A; BD Bioscience), and anti-CTLA4 (intracellular staining) Pe-Cy5 (ECK1; BioLegend).

Statistical analysis

Statistical analyses were performed with R v3.12 software. The statistical tests that were used in each experiment are specified in the corresponding figure legend. Each dataset was assessed for normality using the Shapiro–Wilk normality test. The Wilcoxon–Mann–Whitney *U* test was used to compare two independent groups with non-normal distribution and unequal sample sizes. Paired *T* test was performed to compare the means between two related groups of samples. The linear mixed effects model approach was used for longitudinal or repeated measures comparisons over time. It was also used to adjust for the effect of perinatal factors on the frequency of Vγ9 T cells or Vδ1 T cells during the first month of life. The linear mixed effect model was computed using the lme4 package. Post-hoc comparisons were performed using the Tukey method for multiple comparisons, using the library multcomp. P values are indicated in the figures as follows: ns = not significant, *P < 0.05, **P < 0.01, ***P < 0.001.

Online supplemental material

Two tables and five figures are provided in the online supplementary information. They describe the analysis of γδ T cells by

flow cytometry during the first year of life after preterm birth (Fig. S1), the longitudinal analyses of TCR repertoires after preterm birth (Fig. S2), the phenotypic analysis of γδ T cells by spectral flow cytometry in preterm neonates and infants (Fig. S3), single-cell transcriptome and TCR repertoire data of γδ T cells in longitudinally followed preterm neonates (Fig. S4), and the response of neonatal and adult Vγ9Vδ2 T cells after in vitro HMBPP stimulation (Fig. S5). Table S1 lists the description of TCR cluster features. Table S2 lists information about antibodies used in flow cytometry.

Data availability

Raw single-cell sequencing data is available under NCBI's Gene Expression Omnibus (GSE245131). FASTQ files of TRD and TRG sequences were deposited at NCBI's Sequence Read Archive under the BioProject no. PRJNA1026551.

Acknowledgments

We thank Matthias Ballmaier of the central cell sorting facility and the Genomics platform of the Hannover Medical School for support.

The study was supported by the Deutsche Forschungsgemeinschaft (DFG, German Research Foundation) under Germany's Excellence Strategy—EXC 2155 RESIST—Project ID 390874280 to R. Förster, D. Viemann, and S. Ravens; and the DFG-funded research group FOR2799 Project ID RA3077/1-2 to S. Ravens. S. Pirr and D. Viemann received further funding from the Federal Ministry of Education and Research (PROSPER 01EK2103B and 01EK2103A, respectively) and the DFG to S. Pirr (PI 1512/1-3) and D. Viemann (VI 538/6-3 and VI 538-9-1, the DFG SFB 1583/1 ["DECIDE"] project number 492620490, and the DFG TRR 359 ["PILOT"] project number 491676693). Hannover Medical Research Schools supported X. León-Lara, T. Yang, V. Almeida, and M. Willers.

Author contributions: X. Leon-Lara: Data curation, Formal analysis, Investigation, Methodology, Software, Validation, Visualization, Writing - original draft, Writing - review & editing; A.S. Fichtner: Conceptualization, Data curation, Investigation, Methodology; M. Willers: Investigation; T. Yang: Data curation, Software; K. Schaper: Investigation; L. Riemann: Formal analysis, Software, Writing - review & editing; J. Schoning: Investigation; A. Harms: Investigation; V. Almeida: Investigation; A. Janssen: Investigation; L. Ospina-Quintero: Investigation, Methodology; C. von Kaisenberg: Resources; R. Forster: Writing - review & editing; M. Eberl: Methodology, Writing - review & editing; M.F. Richter: Resources; S. Pirr: Data curation, Writing - review & editing; D. Viemann: Conceptualization, Data curation, Funding acquisition, Methodology, Resources, Supervision, Writing - review & editing; S. Ravens: Conceptualization, Funding acquisition, Project administration, Supervision, Writing - original draft.

Disclosures: S. Pirr reported grants from Deutsche Forschungsgemeinschaft and grants from the German Ministry of Education and Research outside the submitted work. No other disclosures were reported.

Submitted: 30 October 2023
Revised: 6 March 2024
Accepted: 22 April 2024

References

Barisa, M., A.M. Kramer, Y. Majani, D. Moulding, L. Saraiva, M. Bajaj-Elliott, J. Anderson, and K. Gustafsson. 2017. E. coli promotes human Vγ9Vδ2 T cell transition from cytokine-producing bactericidal effectors to professional phagocytic killers in a TCR-dependent manner. *Sci. Rep.* 7:2805. https://doi.org/10.1038/s41598-017-02886-8

Barros-Martins, J., E. Bruni, A.S. Fichtner, M. Cornberg, and I. Prinz. 2022. OMIP-084: 28-color full spectrum flow cytometry panel for the comprehensive analysis of human γδ T cells. *Cytometry A.* 101:856–861. https://doi.org/10.1002/cyto.a.24564

Bolotin, D.A., S. Poslavsky, I. Mitrophanov, M. Shugay, I.Z. Mamedov, E.V. Putintseva, and D.M. Chudakov. 2015. MiXCR: Software for comprehensive adaptive immunity profiling. *Nat. Methods.* 12:380–381. https://doi.org/10.1038/nmeth.3364

Brandes, M., K. Willimann, A.B. Lang, K.-H. Nam, C. Jin, M.B. Brenner, C.T. Morita, and B. Moser. 2003. Flexible migration program regulates γ δ T-cell involvement in humoral immunity. *Blood.* 102:3693–3701. https://doi.org/10.1182/blood-2003-04-1016

Brandes, M., Willimann, K., Moser, B., 2005. Professional Antigen-Presentation Function by Human γδ T Cells. *Science.* 309:264–268. https://doi.org/10.1126/science.1110267

Brodin, P., V. Jojic, T. Gao, S. Bhattacharya, C.J.L. Angel, D. Furman, S. Shen-Orr, C.L. Dekker, G.E. Swan, A.J. Butte, et al. 2015. Variation in the human immune system is largely driven by non-heritable influences. *Cell.* 160:37–47. https://doi.org/10.1016/j.cell.2014.12.020

Cairo, C., N. Longinaker, G. Cappelli, R.G.F. Leke, M.M. Ondo, R. Djokam, J. Fogako, R.J. Leke, B. Sagnia, S. Sosso, et al. 2014. Cord blood Vγ2Vδ2 T cells provide a molecular marker for the influence of pregnancy-associated malaria on neonatal immunity. *J. Infect. Dis.* 209:1653–1662. https://doi.org/10.1093/infdis/jit802

Coffey, F., S.-Y. Lee, T.B. Buus, J.-P.H. Lauritsen, G.W. Wong, M.L. Joachims, L.F. Thompson, J.C. Zúñiga-Pflücker, D.J. Kappes, and D.L. Wiest. 2014. The TCR ligand-inducible expression of CD73 marks γδ lineage commitment and a metastable intermediate in effector specification. *J. Exp. Med.* 211:329–343. https://doi.org/10.1084/jem.20131540

Davenport, M.P., N.L. Smith, and B.D. Rudd. 2020. Building a T cell compartment: How immune cell development shapes function. *Nat. Rev. Immunol.* 20:499–506. https://doi.org/10.1038/s41577-020-0332-3

Davey, M.S., C.R. Willcox, S. Hunter, S.A. Kasatskaya, E.B.M. Remmerswaal, M. Salim, F. Mohammed, F.J. Bemelman, D.M. Chudakov, Y.H. Oo, and B.E. Willcox. 2018. The human Vδ2$^+$ T-cell compartment comprises distinct innate-like Vγ9$^+$ and adaptive Vγ9$^-$ subsets. *Nat. Commun.* 9:1760. https://doi.org/10.1038/s41467-018-04076-0

Davey, M.S., C.R. Willcox, S.P. Joyce, K. Ladell, S.A. Kasatskaya, J.E. McLaren, S. Hunter, M. Salim, F. Mohammed, D.A. Price, et al. 2017. Clonal selection in the human Vδ1 T cell repertoire indicates γδ TCR-dependent adaptive immune surveillance. *Nat. Commun.* 8:14760. https://doi.org/10.1038/ncomms14760

De Rosa, S.C., J.P. Andrus, S.P. Perfetto, J.J. Mantovani, L.A. Herzenberg, L.A. Herzenberg, and M. Roederer. 2004. Ontogeny of γ δ T cells in humans. *J. Immunol.* 172:1637–1645. https://doi.org/10.4049/jimmunol.172.3.1637

Deibel, M.R. Jr., L.K. Riley, M.S. Coleman, M.L. Cibull, S.A. Fuller, and E. Todd. 1983. Expression of terminal deoxynucleotidyl transferase in human thymus during ontogeny and development. *J. Immunol.* 131:195–200. https://doi.org/10.4049/jimmunol.131.1.195

Di Lorenzo, B., S. Ravens, and B. Silva-Santos. 2019. High-throughput analysis of the human thymic Vδ1$^+$ T cell receptor repertoire. *Sci. Data.* 6:115. https://doi.org/10.1038/s41597-019-0118-2

Dijkstra, J.M., and T. Yamaguchi. 2019. Ancient features of the MHC class II presentation pathway, and a model for the possible origin of MHC molecules. *Immunogenetics.* 71:233–249. https://doi.org/10.1007/s00251-018-1090-2

Dowling, D.J., and O. Levy. 2014. Ontogeny of early life immunity. *Trends Immunol.* 35:299–310. https://doi.org/10.1016/j.it.2014.04.007

Eberl, M., M. Hintz, A. Reichenberg, A.-K. Kollas, J. Wiesner, and H. Jomaa. 2003. Microbial isoprenoid biosynthesis and human gammadelta T cell activation. *FEBS Lett.* 544:4–10. https://doi.org/10.1016/s0014-5793(03)00483-6

Eberl, M., and B. Moser. 2009. Monocytes and gammadelta T cells: Close encounters in microbial infection. *Trends Immunol.* 30:562–568. https://doi.org/10.1016/j.it.2009.09.001

Fichtner, A.S., A. Bubke, F. Rampoldi, A. Wilharm, L. Tan, L. Steinbrück, C. Schultze-Florey, C. von Kaisenberg, I. Prinz, T. Herrmann, and S. Ravens. 2020a. TCR repertoire analysis reveals phosphoantigen-induced polyclonal proliferation of Vγ9Vδ2 T cells in neonates and adults. *J. Leukoc. Biol.* 107:1023–1032. https://doi.org/10.1002/JLB.1MA0120-427RR

Fichtner, A.S., S. Ravens, and I. Prinz. 2020b. Human γδ TCR repertoires in health and disease. *Cells.* 9:800. https://doi.org/10.3390/cells9040800

Foss, A., M. Markatou, B. Ray, and A. Heching. 2016. A semiparametric method for clustering mixed data. *Mach. Learn.* 105:419–458. https://doi.org/10.1007/s10994-016-5575-7

Gervassi, A., N. Lejarcegui, S. Dross, A. Jacobson, G. Itaya, E. Kidzeru, S. Gantt, H. Jaspan, and H. Horton. 2014. Myeloid derived suppressor cells are present at high frequency in neonates and suppress in vitro T cell responses. *PLoS One.* 9:e107816. https://doi.org/10.1371/journal.pone.0107816

Gibbons, D.L., S.F.Y. Haque, T. Silberzahn, K. Hamilton, C. Langford, P. Ellis, R. Carr, and A.C. Hayday. 2009. Neonates harbour highly active gammadelta T cells with selective impairments in preterm infants. *Eur. J. Immunol.* 39:1794–1806. https://doi.org/10.1002/eji.200939222

Glatzel, A., D. Wesch, F. Schiemann, E. Brandt, O. Janssen, and D. Kabelitz. 2002. Patterns of chemokine receptor expression on peripheral blood gamma delta T lymphocytes: Strong expression of CCR5 is a selective feature of V delta 2/V gamma 9 gamma delta T cells. *J. Immunol.* 168:4920–4929. https://doi.org/10.4049/jimmunol.168.10.4920

Greenwald, R.J., G.J. Freeman, and A.H. Sharpe. 2005. The B7 family revisited. *Annu. Rev. Immunol.* 23:515–548. https://doi.org/10.1146/annurev.immunol.23.021704.115611

Grosche, L., I. Knippertz, C. König, D. Royzman, A.B. Wild, E. Zinser, H. Sticht, Y.A. Muller, A. Steinkasserer, and M. Lechmann. 2020. The CD83 molecule—an important immune checkpoint. *Front. Immunol.* 11:721. https://doi.org/10.3389/fimmu.2020.00721

Guo, X.J., P. Dash, J.C. Crawford, E.K. Allen, A.E. Zamora, D.F. Boyd, S. Duan, R. Bajracharya, W.A. Awad, N. Apiwattanakul, et al. 2018. Lung γδ T cells mediate protective responses during neonatal influenza infection that are associated with type 2 immunity. *Immunity.* 49:531–544.e6. https://doi.org/10.1016/j.immuni.2018.07.011

Harmon, C., A. Zaborowski, H. Moore, P. St Louis, K. Slattery, D. Duquette, J. Scanlan, H. Kane, B. Kunkemoeller, C.L. McIntyre, et al. 2023. γδ T cell dichotomy with opposing cytotoxic and wound healing functions in human solid tumors. *Nat. Cancer.* 4:1122–1137. https://doi.org/10.1038/s43018-023-00589-w

He, Y.-M., X. Li, M. Perego, Y. Nefedova, A.V. Kossenkov, E.A. Jensen, V. Kagan, Y.-F. Liu, S.-Y. Fu, Q.-J. Ye, et al. 2018. Transitory presence of myeloid-derived suppressor cells in neonates is critical for control of inflammation. *Nat. Med.* 24:224–231. https://doi.org/10.1038/nm.4467

Herrmann, T., and M.M. Karunakaran. 2022. Butyrophilins: γδ T cell receptor ligands, immunomodulators and more. *Front. Immunol.* 13:876493. https://doi.org/10.3389/fimmu.2022.876493

Holmen Olofsson, G., M. Idorn, A.M. Carnaz Simões, P. Aehnlich, S.K. Skadborg, E. Noessner, R. Debets, B. Moser, Ö. Met, and P. Thor Straten. 2021. Vγ9Vδ2 T cells concurrently kill cancer cells and cross-present tumor antigens. *Front. Immunol.* 12:645131. https://doi.org/10.3389/fimmu.2021.645131

Howard, J., S. Loizon, C.J. Tyler, D. Duluc, B. Moser, M. Mechain, A. Duvignaud, D. Malvy, M. Troye-Blomberg, J.-F. Moreau, et al. 2017. The antigen-presenting potential of Vγ9Vδ2 T cells during plasmodium falciparum blood-stage infection. *J. Infect. Dis.* 215:1569–1579. https://doi.org/10.1093/infdis/jix149

Hsu, H., S. Boudova, G. Mvula, T.H. Divala, R.G. Mungwira, C. Harman, M.K. Laufer, C.D. Pauza, and C. Cairo. 2016. Prolonged PD1 expression on neonatal Vδ2 lymphocytes dampens proinflammatory responses: Role of epigenetic regulation. *J. Immunol.* 197:1884–1892. https://doi.org/10.4049/jimmunol.1600284

Hsu, H., S. Boudova, G. Mvula, T.H. Divala, D. Rach, R.G. Mungwira, F. Boldrin, G. Degiacomi, R. Manganelli, M.K. Laufer, and C. Cairo. 2021. Age-related changes in PD-1 expression coincide with increased cytotoxic potential in Vδ2 T cells during infancy. *Cell. Immunol.* 359:104244. https://doi.org/10.1016/j.cellimm.2020.104244

Kan, B., H.R. Razzaghian, and P.M. Lavoie. 2016. An immunological perspective on neonatal sepsis. *Trends Mol. Med.* 22:290–302. https://doi.org/10.1016/j.molmed.2016.02.001

Lechmann, M., D.J.E.B. Krooshoop, D. Dudziak, E. Kremmer, C. Kuhnt, C.G. Figdor, G. Schuler, and A. Steinkasserer. 2001. The extracellular domain of CD83 inhibits dendritic cell-mediated T cell stimulation and binds to a ligand on dendritic cells. *J. Exp. Med.* 194:1813–1821. https://doi.org/10.1084/jem.194.12.1813

Liuzzi, A.R., A. Kift-Morgan, M. Lopez-Anton, I.M. Friberg, J. Zhang, A.C. Brook, G.W. Roberts, K.L. Donovan, C.S. Colmont, M.A. Toleman, et al. 2016. Unconventional human T cells accumulate at the site of infection in response to microbial ligands and induce local tissue remodeling. *J. Immunol.* 197:2195–2207. https://doi.org/10.4049/jimmunol.1600990

Ma, L., M. Papadopoulou, M. Taton, F. Genco, A. Marchant, V. Meroni, and D. Vermijlen. 2021. Effector Vγ9Vδ2 T cell response to congenital Toxoplasma gondii infection. *JCI Insight.* 6:e138066. https://doi.org/10.1172/jci.insight.138066

Mariβen, J., Haiß, A., Meyer, C., Van Rossum, T., Bünte, L.M., Frommhold, D., Gille, C., Goedicke-Fritz, S., Göpel, W., Hudalla, H., et al, 2019. Efficacy of Bifidobacterium longum, B. infantis and Lactobacillus acidophilus probiotics to prevent gut dysbiosis in preterm infants of 28+0-32+6 weeks of gestation: a randomised, placebo-controlled, double-blind, multicentre trial: the PRIMAL Clinical Study protocol. *BMJ Open.* 9:e032617. https://doi.org/10.1136/bmjopen-2019-032617

McMurray, J.L., A. von Borstel, T.E. Taher, E. Syrimi, G.S. Taylor, M. Sharif, J. Rossjohn, E.B.M. Remmerswaal, F.J. Bemelman, F.A. Vieira Braga, et al. 2022. Transcriptional profiling of human Vδ1 T cells reveals a pathogen-driven adaptive differentiation program. *Cell Rep.* 39:110858. https://doi.org/10.1016/j.celrep.2022.110858

McVay, L.D., S.S. Jaswal, C. Kennedy, A. Hayday, and S.R. Carding. 1998. The generation of human gammadelta T cell repertoires during fetal development. *J. Immunol.* 160:5851–5860. https://doi.org/10.4049/jimmunol.160.12.5851

Meuter, S., M. Eberl, and B. Moser. 2010. Prolonged antigen survival and cytosolic export in cross-presenting human gammadelta T cells. *Proc. Natl. Acad. Sci. USA.* 107:8730–8735. https://doi.org/10.1073/pnas.1002769107

Morita, C.T., C. Jin, G. Sarikonda, and H. Wang. 2007. Nonpeptide antigens, presentation mechanisms, and immunological memory of human Vgamma2Vdelta2 T cells: Discriminating friend from foe through the recognition of prenyl pyrophosphate antigens. *Immunol. Rev.* 215:59–76. https://doi.org/10.1111/j.1600-065X.2006.00479.x

Notarangelo, L.D., M.-S. Kim, J.E. Walter, and Y.N. Lee. 2016. Human RAG mutations: Biochemistry and clinical implications. *Nat. Rev. Immunol.* 16:234–246. https://doi.org/10.1038/nri.2016.28

Odumade, O.A., M.A. Weinreich, S.C. Jameson, and K.A. Hogquist. 2010. Krüppel-like factor 2 regulates trafficking and homeostasis of gammadelta T cells. *J. Immunol.* 184:6060–6066. https://doi.org/10.4049/jimmunol.1000511

Olin, A., E. Henckel, Y. Chen, T. Lakshmikanth, C. Pou, J. Mikes, A. Gustafsson, A.K. Bernhardsson, C. Zhang, K. Bohlin, and P. Brodin. 2018. Stereotypic immune system development in newborn children. *Cell.* 174:1277–1292.e14. https://doi.org/10.1016/j.cell.2018.06.045

Papadopoulou, M., T. Dimova, M. Shey, L. Briel, H. Veldtsman, N. Khomba, H. Africa, M. Steyn, W.A. Hanekom, T.J. Scriba, et al. 2020. Fetal public Vγ9Vδ2 T cells expand and gain potent cytotoxic functions early after birth. *Proc. Natl. Acad. Sci. USA.* 117:18638–18648. https://doi.org/10.1073/pnas.1922595117

Papadopoulou, M., P. Tieppo, N. McGovern, F. Gosselin, J.K.Y. Chan, G. Goetgeluk, N. Dauby, A. Cogan, C. Donner, F. Ginhoux, et al. 2019. TCR sequencing reveals the distinct development of fetal and adult human Vγ9Vδ2 T cells. *J. Immunol.* 203:1468–1479. https://doi.org/10.4049/jimmunol.1900592

Parker, C.M., V. Groh, H. Band, S.A. Porcelli, C. Morita, M. Fabbi, D. Glass, J.L. Strominger, and M.B. Brenner. 1990. Evidence for extrathymic changes in the T cell receptor gamma/delta repertoire. *J. Exp. Med.* 171:1597–1612. https://doi.org/10.1084/jem.171.5.1597

Perriman, L., N. Tavakolinia, S. Jalali, S. Li, P.F. Hickey, D. Amann-Zalcenstein, W.W.H. Ho, T.M. Baldwin, A.T. Piers, I.E. Konstantinov, et al. 2023. A three-stage developmental pathway for human Vγ9Vδ2 T cells within the postnatal thymus. *Sci. Immunol.* 8:eabo4365. https://doi.org/10.1126/sciimmunol.abo4365

Pizzolato, G., H. Kaminski, M. Tosolini, D.-M. Franchini, F. Pont, F. Martins, C. Valle, D. Labourdette, S. Cadot, A. Quillet-Mary, et al. 2019. Single-cell RNA sequencing unveils the shared and the distinct cytotoxic hallmarks of human TCRVδ1 and TCRVδ2 γδ T lymphocytes. *Proc. Natl. Acad. Sci. USA*. 116:11906–11915. https://doi.org/10.1073/pnas.1818488116

Rahman Qazi, K., G.B. Jensen, M. van der Heiden, S. Björkander, G. Marchini, M.C. Jenmalm, T. Abrahamsson, and E. Sverremark-Ekström. 2021. Extreme prematurity and sepsis strongly influence frequencies and functional characteristics of circulating γδ T and natural killer cells. *Clin. Transl. Immunol.* 10:e1294. https://doi.org/10.1002/cti2.1294

Ravens, S., A.S. Fichtner, M. Willers, D. Torkornoo, S. Pirr, J. Schöning, M. Deseke, I. Sandrock, A. Bubke, A. Wilharm, et al. 2020. Microbial exposure drives polyclonal expansion of innate γδ T cells immediately after birth. *Proc. Natl. Acad. Sci. USA*. 117:18649–18660. https://doi.org/10.1073/pnas.1922588117

Ravens, S., C. Schultze-Florey, S. Raha, I. Sandrock, M. Drenker, L. Oberdörfer, A. Reinhardt, I. Ravens, M. Beck, R. Geffers, et al. 2017. Human γδ T cells are quickly reconstituted after stem-cell transplantation and show adaptive clonal expansion in response to viral infection. *Nat. Immunol.* 18: 393–401. https://doi.org/10.1038/ni.3686

Reis, B.S., Darcy, P.W., Khan, I.Z., Moon, C.S., Kornberg, A.E., Schneider, V.S., Alvarez, Y., Eleso, O., Zhu, C., Schernthanner, M., et al, 2022. TCR-Vγδ usage distinguishes protumor from antitumor intestinal γδ T cell subsets. *Science*. 377:276–284. https://doi.org/10.1126/science.abj8695

Ribot, J.C., S.T. Ribeiro, D.V. Correia, A.E. Sousa, and B. Silva-Santos. 2014. Human γδ thymocytes are functionally immature and differentiate into cytotoxic type 1 effector T cells upon IL-2/IL-15 signaling. *J. Immunol.* 192:2237–2243. https://doi.org/10.4049/jimmunol.1303119

Sagar, P., M. Pokrovskii, J.S. Herman, S. Naik, E. Sock, P. Zeis, U. Lausch, M. Wegner, Y. Tanriver, D.R. Littman, and D. Grün. 2020. Deciphering the regulatory landscape of fetal and adult γδ T-cell development at single-cell resolution. *EMBO J.* 39:e104159. https://doi.org/10.15252/embj.2019104159

Sanchez Sanchez, G., M. Papadopoulou, A. Azouz, Y. Tafesse, A. Mishra, J.K.Y. Chan, Y. Fan, I. Verdebout, S. Porco, F. Libert, et al. 2022. Identification of distinct functional thymic programming of fetal and pediatric human γδ thymocytes via single-cell analysis. *Nat. Commun.* 13:5842. https://doi.org/10.1038/s41467-022-33488-2

Sanchez Sanchez, G., Y. Tafesse, M. Papadopoulou, and D. Vermijlen. 2023. Surfing on the waves of the human γδ T cell ontogenic sea. *Immunol. Rev.* 315:89–107. https://doi.org/10.1111/imr.13184

Shugay, M., D.V. Bagaev, M.A. Turchaninova, D.A. Bolotin, O.V. Britanova, E.V. Putintseva, M.V. Pogorelyy, V.I. Nazarov, I.V. Zvyagin, V.I. Kirgizova, et al. 2015. VDJtools: Unifying post-analysis of T cell receptor repertoires. *PLoS Comput. Biol.* 11:e1004503. https://doi.org/10.1371/journal.pcbi.1004503

Tan, L., A.S. Fichtner, E. Bruni, I. Odak, I. Sandrock, A. Bubke, A. Borchers, C. Schultze-Florey, C. Koenecke, R. Förster, et al. 2021. A fetal wave of human type 3 effector γδ cells with restricted TCR diversity persists into adulthood. *Sci. Immunol.* 6:eabf0125. https://doi.org/10.1126/sciimmunol.abf0125

Tibshirani, R., and G. Walther. 2005. Cluster validation by prediction strength. *J. Comput. Graph. Stat.* 14:511–528. https://doi.org/10.1198/106186005X59243

Tieppo, P., M. Papadopoulou, D. Gatti, N. McGovern, J.K.Y. Chan, F. Gosselin, G. Goetgeluk, K. Weening, L. Ma, N. Dauby, et al. 2020. The human fetal thymus generates invariant effector γδ T cells. *J. Exp. Med.* 217: jem.20190580. https://doi.org/10.1084/jem.20190580

Torow, N., T.W. Hand, and M.W. Hornef. 2023. Programmed and environmental determinants driving neonatal mucosal immune development. *Immunity*. 56:485–499. https://doi.org/10.1016/j.immuni.2023.02.013

Tuengel, J., S. Ranchal, A. Maslova, G. Aulakh, M. Papadopoulou, S. Drissler, B. Cai, C. Mohsenzadeh-Green, H. Soudeyns, S. Mostafavi, et al. 2021. Characterization of adaptive-like γδ T cells in Ugandan infants during primary cytomegalovirus infection. *Viruses*. 13:1987. https://doi.org/10.3390/v13101987

Tyler, C.J., N.E. McCarthy, J.O. Lindsay, A.J. Stagg, B. Moser, and M. Eberl. 2017. Antigen-presenting human γδ T cells promote intestinal CD4$^+$ T cell expression of IL-22 and mucosal release of calprotectin. *J. Immunol.* 198:3417–3425. https://doi.org/10.4049/jimmunol.1700003

van der Heiden, M., S. Björkander, K. Rahman Qazi, J. Bittmann, L. Hell, M.C. Jenmalm, G. Marchini, D. Vermijlen, T. Abrahamsson, C. Nilsson, and E. Sverremark-Ekström. 2020. Characterization of the γδ T-cell compartment during infancy reveals clear differences between the early neonatal period and 2 years of age. *Immunol. Cell Biol.* 98:79–87. https://doi.org/10.1111/imcb.12303

van der Poll, T., M. Shankar-Hari, and W.J. Wiersinga. 2021. The immunology of sepsis. *Immunity*. 54:2450–2464. https://doi.org/10.1016/j.immuni.2021.10.012

Vermijlen, D., M. Brouwer, C. Donner, C. Liesnard, M. Tackoen, M. Van Rysselberge, N. Twité, M. Goldman, A. Marchant, and F. Willems. 2010. Human cytomegalovirus elicits fetal gammadelta T cell responses in utero. *J. Exp. Med.* 207:807–821. https://doi.org/10.1084/jem.20090348

Vermijlen, D., P. Ellis, C. Langford, A. Klein, R. Engel, K. Willimann, H. Jomaa, A.C. Hayday, and M. Eberl. 2007. Distinct cytokine-driven responses of activated blood gammadelta T cells: Insights into unconventional T cell pleiotropy. *J. Immunol.* 178:4304–4314. https://doi.org/10.4049/jimmunol.178.7.4304

Wang, L., A. Hückelhoven, J. Hong, N. Jin, J. Mani, B.A. Chen, M. Schmitt, and A. Schmitt. 2016. Standardization of cryopreserved peripheral blood mononuclear cells through a resting process for clinical immunomonitoring--Development of an algorithm. *Cytometry A*. 89: 246–258. https://doi.org/10.1002/cyto.a.22813

Yang, J., M. Zou, X. Chu, S. Floess, Y. Li, M. Delacher, and J. Huehn. 2022. Inflammatory perturbations in early life long-lastingly shape the transcriptome and TCR repertoire of the first wave of regulatory T cells. *Front. Immunol.* 13:991671. https://doi.org/10.3389/fimmu.2022.991671

JEM

Supplemental material

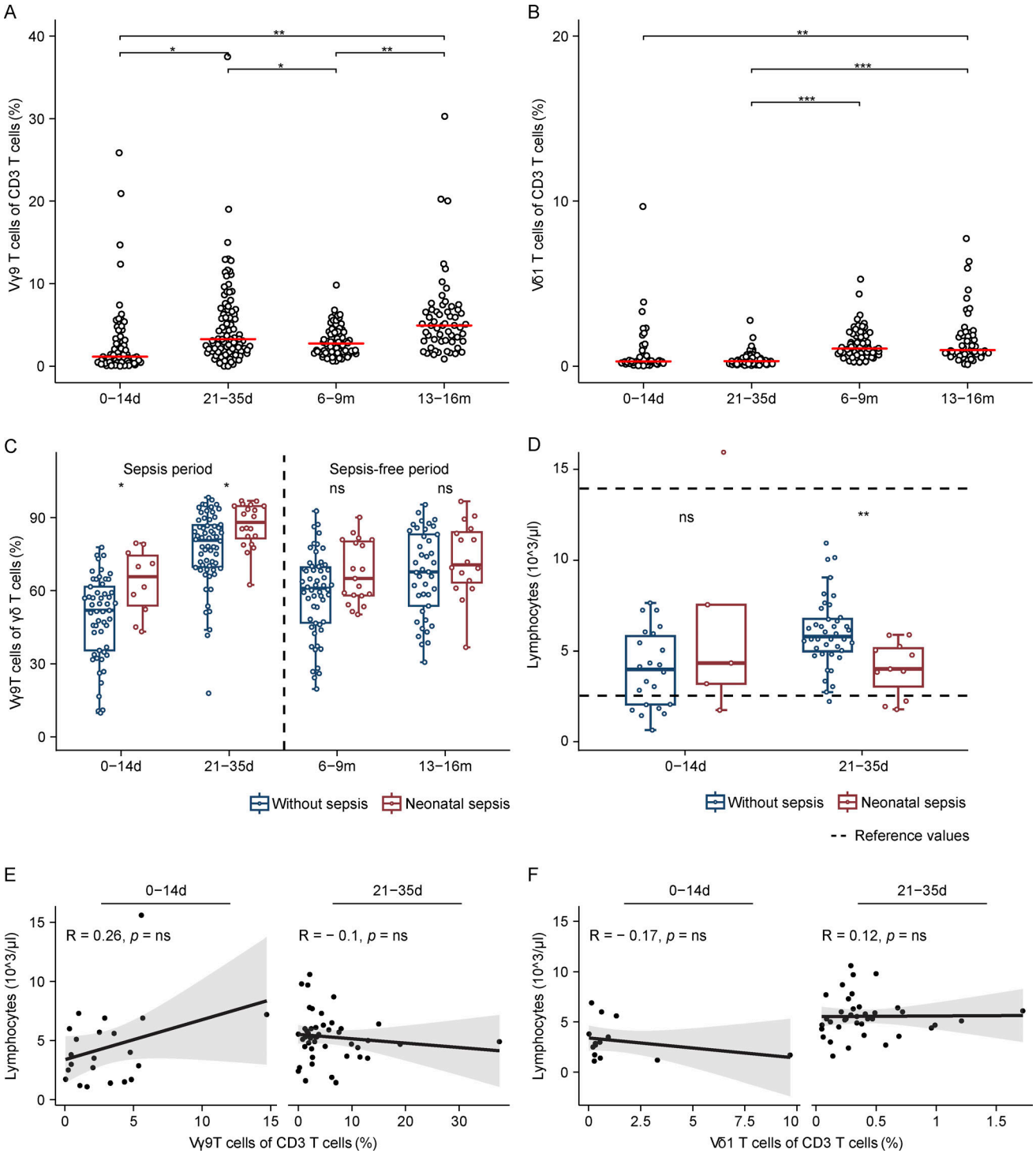

Figure S1. **Longitudinal flow cytometric analyses of γδ T cells during the first year of life. (A and B)** Frequency per donor of (A) Vγ9 T cells or (B) Vδ1 T cells among CD3 T cells by FACS at 0–14 days (d), 21–35 days, 6–9 mo (m), and 13–16 mo after preterm birth. The red bar indicates the median value. **(C)** Box plots of the frequency of Vγ9 T cells among γδ T cells in relation to the diagnosis of sepsis during the neonatal period. **(D)** Box plots of the absolute counts of total lymphocyte populations from peripheral blood of preterm infants with and without sepsis during the neonatal period. **(E and F)** Correlations of lymphocyte cell count with frequency of Vγ9 T cells (E) or Vδ1 T cells (F) among CD3 T cells at 0–14 days (d) or 21–35 d. P values were determined by linear mixed effects modeling (A and B) or Mann–Whitney *U* test (C and D). R and P values were determined by Spearman correlation test (E and F); ns = not significant, *P < 0.05, **P < 0.01, ***P < 0.001.

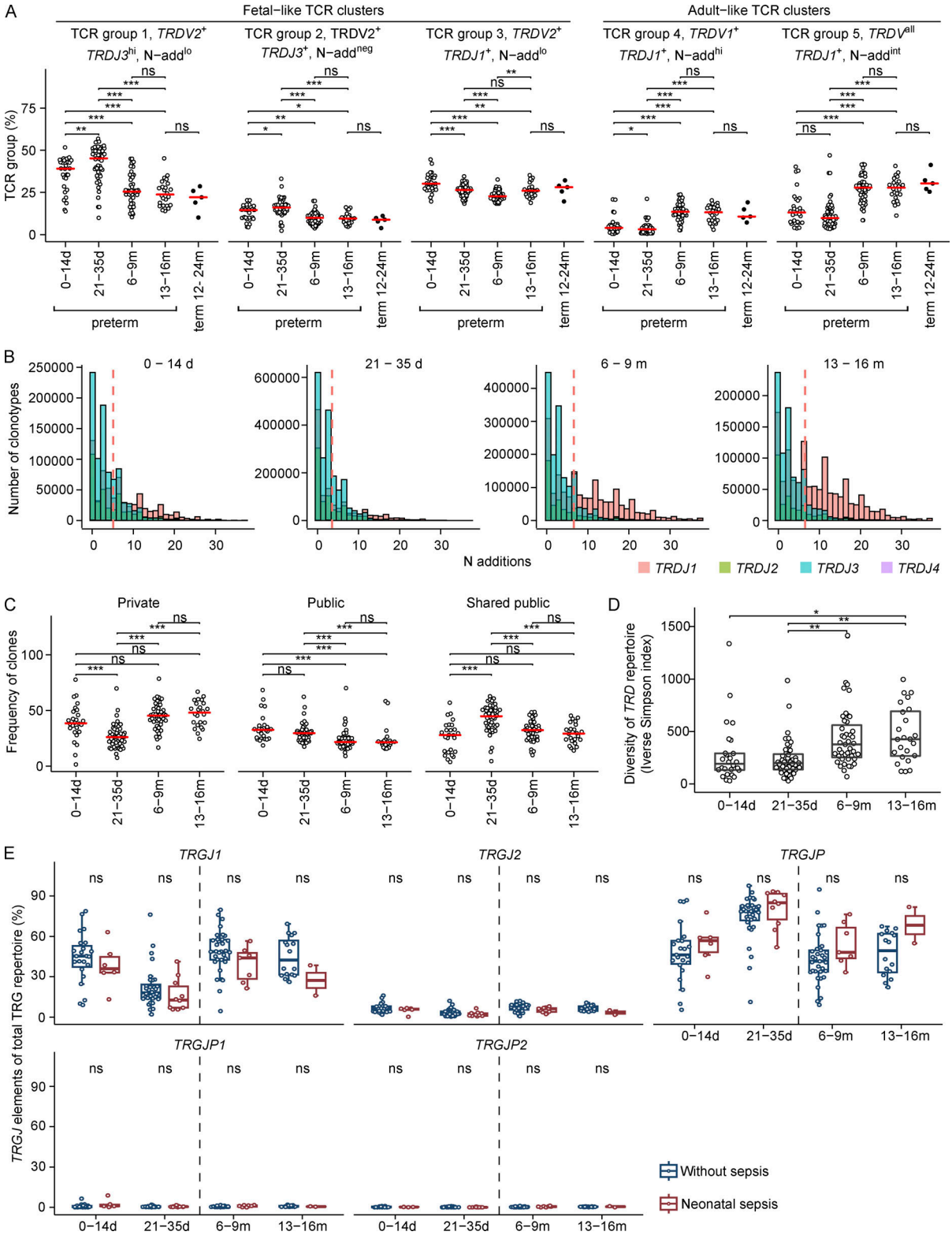

Figure S2. **Longitudinal bulk TCR-seq of γδ T cells during the first year of life. (A)** The total TRD repertoire of FACS-sorted γδ T cells from 58 preterm infants at four time points during the first year of life and five term infants aged 12–24 mo was clustered based on V(D)J characteristics, resulting in five TCR groups. Frequency of each TCR group was calculated per infant at the indicated time points after preterm birth and in term infants at 12–24 mo of age. **(B)** Histogram showing the introduction of random nucleotides (N additions) distribution of the clones per time point, colored by *TRDJ* usage. **(C)** Frequency of private, public, and shared public TRD clones per infant at the respective time points. **(D)** Box plots of the diversity index of the TRD repertoire at the indicated time points. **(E)** Box plots of the *TRGJP* gene element usage in the TRG repertoire at the respective time points after preterm birth in relation to the diagnosis of sepsis in the neonatal period. **(A and C)** The median value is indicated with a red bar. P values were determined by linear mixed effect modeling with multiple comparisons by Tukey (A, C, and D) or Mann–Whitney *U* test (E); ns = not significant, *P < 0.05, **P < 0.01, ***P < 0.001.

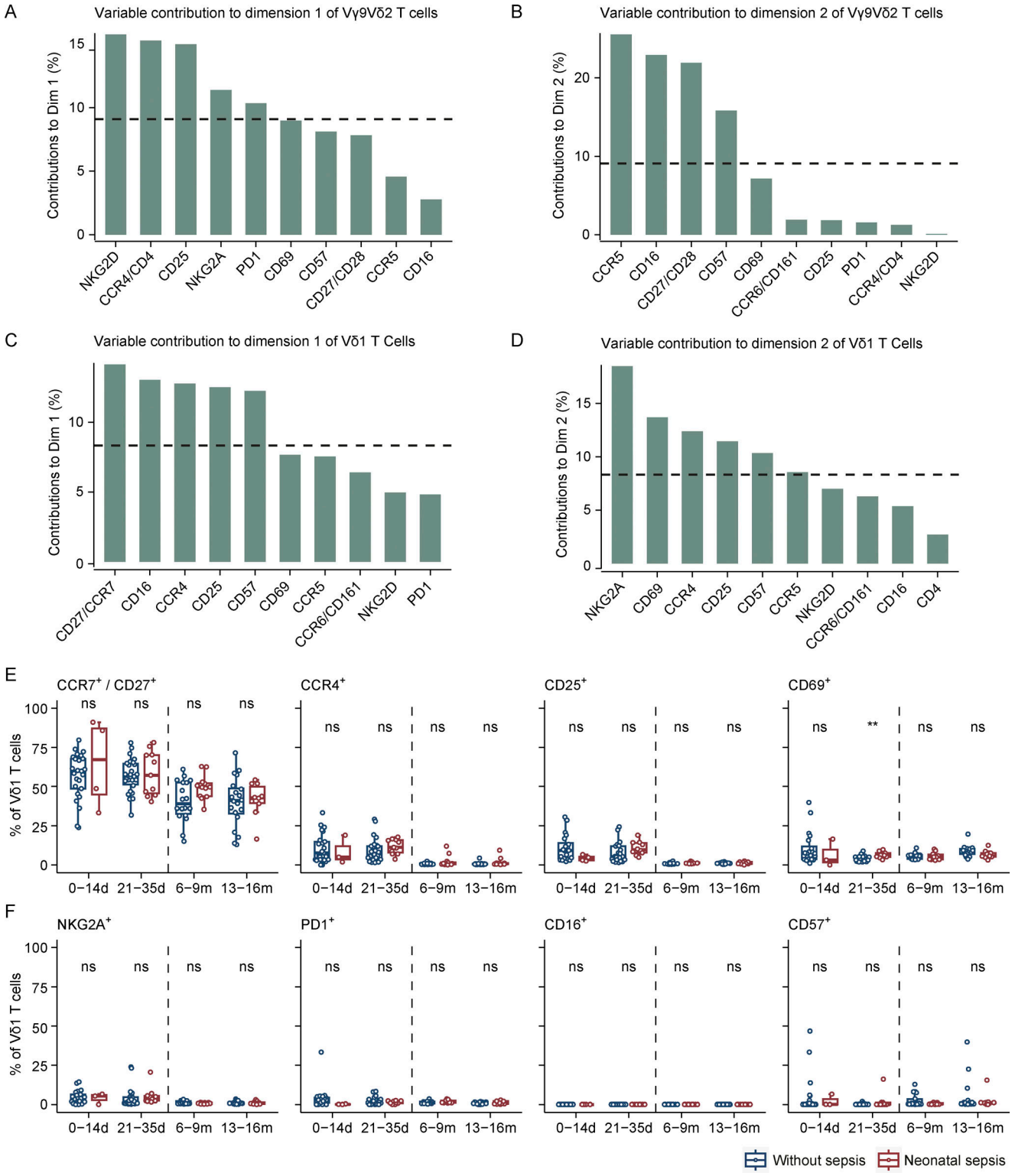

Figure S3. **Longitudinal surface marker profiles of γδ T cells during the first year of life. (A–D)** Contribution of the top 10 variables to the (A) dimension 1 (Dim1) or (B) dimension 2 (Dim2) of the PCA for Vγ9Vδ2 T cells, and the (C) Dim1 or (D) Dim2 of the PCA for Vδ1 T cells. The dashed line indicates the expected average contribution, a variable with a contribution above this line was considered as an important contributor to the dimension. **(E and F)** Box plots of the frequency of (E) CD27, CCR7 co-expression, CCR4, CD25, CD69, (F) NKG2A, PD1, CD16, or CD57 on Vδ1 T cells per donor by FACS at four time points after preterm birth in infants diagnosed with and without neonatal sepsis. P values were determined by Mann–Whitney *U* test (E and F); ns = not significant, **P < 0.01.

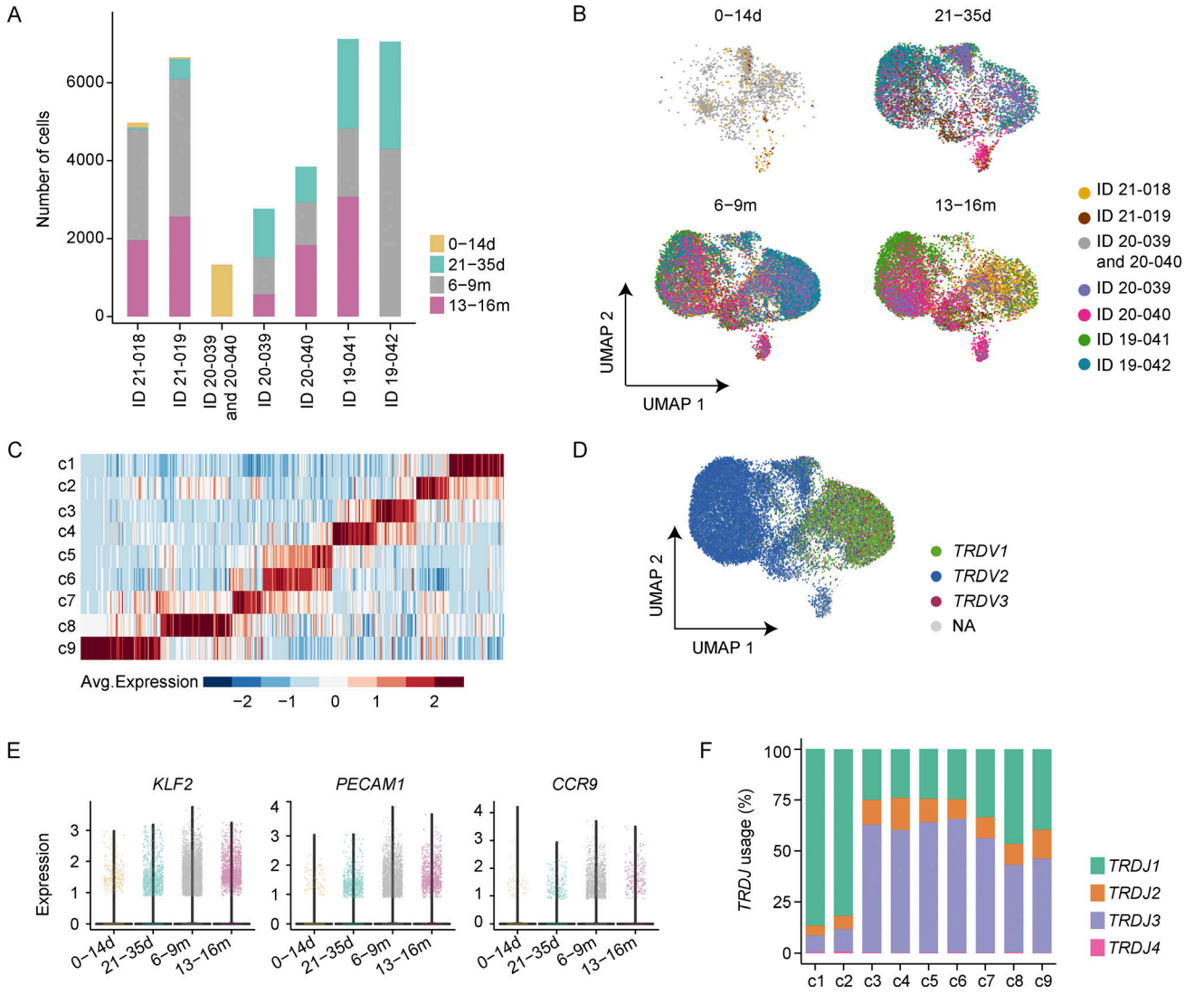

Figure S4. **Longitudinal single-cell transcriptome and TCR repertoire analysis of γδ T cells in preterm infants. (A)** Bar plots of the absolute number of γδ T cells from each donor that were considered for the analysis, colored by the age at sampling. **(B)** UMAP visualization of the γδ T cell scRNA-seq dataset from the infants at the different time points, color-coded by the donor. **(C)** Heat map showing the averaged expression values of the top 100 DEGs (columns) between clusters (rows). **(D)** UMAP visualization of the scTCR-seq dataset showing the *TRDV* gene usage (NA: *TRDV* data not available). **(E)** Violin plots of the *KLF2*, *PECAM1*, or *CCR9* expression at 0–14 days (yellow), 21–35 days (green), 6–9 mo (gray), or 13–16 mo (pink). **(F)** Bar plots of the frequency of TRDJ gene element segment usage in each cluster. Cells without a paired γδTCR were excluded.

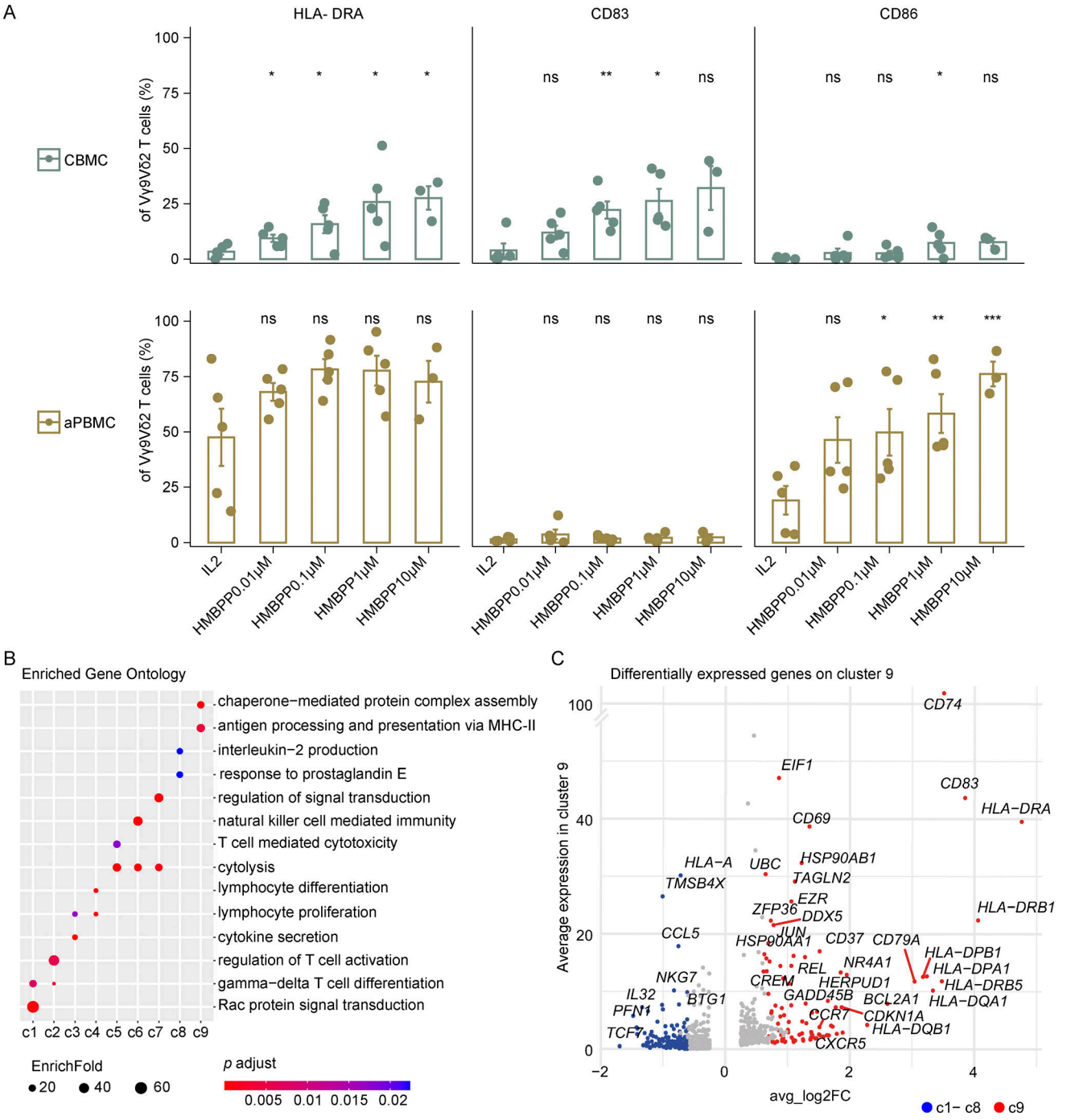

Figure S5. **Adult and neonatal Vγ9Vδ2 T cells acquire different surface marker phenotypes in response to HMBPP stimulus. (A)** Frequency of HLA-DRA, CD83, and CD86 surface expression on Vγ9Vδ2 T cells from CBMCs, and adult PBMC (aPBMC) after 7 days of different doses of HMBPP or IL-2 only stimulation measured by flow cytometry in two independent experiments. Bar plots represent the mean ± standard error. P values were determined by paired *t* test using IL-2 condition as the reference; ns = not significant, *P < 0.05, **P < 0.01, ***P < 0.001. **(B)** GO enrichment analysis of the upregulated differential expressed genes from the respective cluster (c1–c9). **(C)** Volcano plot shows the average expression of the DEGs between c9 in comparison to the rest of the clusters (c1–c8).

Provided online are Table S1 and Table S2. Table S1 lists features of TRD repertoire groups. Table S2 shows the antibody list for spectral flow cytometry.